
Superconducting Polarons and Bipolarons

A. S. Alexandrov

Department of Physics, Loughborough University, Loughborough LE11 3TU,
United Kingdom

a.s.alexandrov@lboro.ac.uk

Summary. The seminal work by Bardeen, Cooper and Schrieffer (BCS) extended further by Eliashberg to the intermediate coupling regime solved one of the major scientific problems of Condensed Matter Physics in the last century. The BCS theory provides qualitative and in many cases quantitative descriptions of low-temperature superconducting metals and their alloys, and some novel high-temperature superconductors like magnesium diboride. The theory has been extended by us to the strong-coupling regime where carriers are small lattice polarons and bipolarons. Here I review the multi-polaron strong-coupling theory of superconductivity. Attractive electron correlations, prerequisite to any superconductivity, are caused by an almost unretarded electron-phonon (e-ph) interaction sufficient to overcome the direct Coulomb repulsion in this regime. Low energy physics is that of small polarons and bipolarons, which are real-space electron (hole) pairs dressed by phonons. They are itinerant quasiparticles existing in the Bloch states at temperatures below the characteristic phonon frequency. Since there is almost no retardation (i.e. no Tolmachev-Morel-Anderson logarithm) reducing the Coulomb repulsion, e-ph interactions should be relatively strong to overcome the direct Coulomb repulsion, so carriers *must* be polaronic to form pairs in novel superconductors. I identify the long-range Fröhlich electron-phonon interaction as the most essential for pairing in superconducting cuprates. A number of key observations have been predicted or explained with polarons and bipolarons including unusual isotope effects and upper critical fields, normal state (pseudo)gaps and kinetic properties, normal state diamagnetism, and giant proximity effects. These and many other observations provide strong evidence for a novel state of electronic matter in layered cuprates, which is a charged Bose-liquid of small mobile bipolarons.

1 Introduction

While a single polaron problem has been actively researched for a long time (for reviews see ref. [1, 2, 4, 5, 6, 7, 8, 9, 10] and the present volume.), multi-polaron physics has gained particular attention in the last two decades. For weak electron-phonon coupling, $\lambda < 1$, and the adiabatic limit, $\omega/E_F \ll 1$), Migdal theory describes electron dynamics in the normal Fermi-liquid state

[11], and BCS-Eliashberg theory in the superconducting state [12, 13] (here and further I use $\hbar = c = k_B = 1$). While the electron-phonon (e-ph) interaction is weak Migdal's theorem is perfectly applied. The theorem proves that the contribution of diagrams with "crossing" phonon lines (so called "vertex" corrections) is small if the parameter $\lambda\omega/E_F$ is small, where λ is the dimensionless (BCS) e-ph coupling constant, ω is the characteristic phonon frequency, and E_F is the Fermi energy. Neglecting the vertex corrections, Migdal [11] calculated the renormalized electron mass as $m^* = m_0(1 + \lambda)$ (near the Fermi level), where m_0 is the band mass in the absence of e-ph interaction, and Eliashberg [13] extended Migdal's theory to describe the BCS superconducting state at intermediate values of $\lambda < 1$. Later on many researchers applied Migdal-Eliashberg theory with λ even larger than 1 (see, for example, Ref. [14], and references therein). With increasing strength of interaction and increasing phonon frequency, ω , finite bandwidth [15, 16] and vertex corrections [17] become increasingly important. But unexpectedly for many researchers who applied the non-crossing approximation even at $\lambda > 1$ we have found that the Migdal-BCS-Eliashberg theory (with or without vertex corrections) breaks down entirely at $\lambda \sim 1$ for any value of the adiabatic ratio ω/E_F since the bandwidth is narrowed and the Fermi energy, E_F is renormalised down exponentially so the effective parameter $\lambda\omega/E_F$ becomes large [18].

The electron-phonon coupling constant λ is about the ratio of the electron-phonon interaction energy E_p to the half bandwidth $D \approx N(E_F)^{-1}$, where $N(E)$ is the density of electron states in a rigid lattice. One expects [18] that when the coupling is strong, $\lambda > 1$, all electrons in the bare Bloch band are "dressed" by phonons since their kinetic energy ($< D$) is small compared with the potential energy due to the local lattice deformation, E_p , caused by electrons. In this strong coupling regime the canonical Lang-Firsov transformation [19] can be used to determine the properties of the system. Under certain conditions [20, 21, 22, 23], the multi-polaron system is metallic but with polaronic carriers rather than bare electrons. This regime is beyond Migdal-Eliashberg theory, where the effective mass approximation is used and the electron bandwidth is infinite. In particular, the small polaron regime cannot be reached by summation of the standard Feynman-Dyson perturbation diagrams using a translation-invariant Green's function $G(\mathbf{r}, \mathbf{r}', \tau) = G(\mathbf{r} - \mathbf{r}', \tau)$ with the Fourier transform $G(\mathbf{k}, \Omega)$ prior to solving the Dyson equations on a discrete lattice. This assumption excludes the possibility of local violation of the translational symmetry [24] due to the lattice deformation in any order of the Feynman-Dyson perturbation theory similar to the absence of the anomalous (Bogoliubov) averages in any order of perturbation theory [11]. To enable electrons to relax into the lowest polaronic band, one has to introduce an infinitesimal translation-noninvariant potential, which should be set zero only in the final solution obtained by the summation of Feynman diagrams for the Fourier transform $G(\mathbf{k}, \mathbf{k}', \Omega)$ of $G(\mathbf{r}, \mathbf{r}', \tau)$ rather than for $G(\mathbf{k}, \Omega)$ [15]. As in the case of the off-diagonal superconducting order parameter, the off-

diagonal terms of the Green function, in particular the Umklapp terms with $\mathbf{k}' = \mathbf{k} + \mathbf{G}$, drive the system into a small polaron ground state at sufficiently large coupling. Setting the translation-noninvariant potential to zero in the solution of the equations of motion restores the translation symmetry but in a polaron band rather than in the bare electron band, which turns out to be an excited state.

Alternatively, one can work with momentum eigenstates throughout the whole coupling region, but taking into account the finite electron bandwidth from the very beginning. In recent years many numerical, and analytical studies have confirmed the conclusion [18], that the Migdal-Eliashberg theory breaks down at $\lambda \geq 1$ (see, for example Refs. [25, 26, 27, 28, 29, 30, 31, 32, 33, 34, 35, 36, 37, 38] and contributions to this book). With increasing phonon frequency the range of validity of the $1/\lambda$ polaron expansion extends to smaller values of λ [39]. As a result, the region of applicability of the Migdal-Eliashberg approach (even with vertex corrections) shrinks to smaller values of the coupling, $\lambda < 1$, with increasing ω . Strong correlations between carriers reduce this region further (see [30]).

Carriers in the fascinating advanced materials are strongly coupled with high-frequency optical phonons, making small polarons and non-adiabatic effects relevant for high-temperature superconductivity, colossal magnetoresistance phenomenon, and molecular electronic devices (see Part III). Indeed the characteristic phonon energies 0.05 – 0.2 eV in cuprates, manganites and in many organic materials are of the same order as generally accepted values of the hopping integrals 0.1 – 0.3 eV.

As reviewed in this book lattice polarons are different from ordinary electrons in many aspects, but perhaps one of the most remarkable difference is found in their superconducting properties. By extending the BCS theory towards the strong interaction between electrons and ion vibrations, a charged Bose gas (CBG) of tightly bound small bipolarons was predicted by us [41] with a further prediction that high critical temperature T_c is found in the crossover region of the e-ph interaction strength from the BCS-like *polaronic* to *bipolaronic* superconductivity [18]. This contribution describes what happens to the conventional BCS theory when the electron-phonon coupling becomes strong. The author's particular view of cuprates is also presented.

2 Electron-phonon and Coulomb interactions in Wannier representation

For doped semiconductors and metals with a strong electron-phonon interaction it is convenient to transform the Bloch states $|\mathbf{k}\rangle$ to the site (Wannier) states $|\mathbf{m}\rangle$ using the canonical linear transformation of the electron operators,

$$c_i = \frac{1}{\sqrt{N}} \sum_{\mathbf{k}} e^{i\mathbf{k}\cdot\mathbf{m}} c_{\mathbf{k}s}, \quad (1)$$

where $i = (\mathbf{m}, s)$ includes both site \mathbf{m} and spin s quantum numbers, and N is the number of sites in a crystal. In the site representation the electron kinetic energy takes the following form

$$H_e = \sum_{i,j} [T(\mathbf{m} - \mathbf{m}')\delta_{ss'} - \mu\delta_{ij}] c_i^\dagger c_j, \quad (2)$$

where

$$T(\mathbf{m}) = \frac{1}{N} \sum_{\mathbf{k}} E_{\mathbf{k}} e^{i\mathbf{k}\cdot\mathbf{m}}$$

is the bare hopping integral in the rigid lattice, μ is the chemical potential, $j = (\mathbf{n}, s')$, and $E_{\mathbf{k}}$ is the bare Bloch band dispersion.

The electron-phonon and Coulomb interactions acquire simple forms in the Wannier representation, if their matrix elements in the momentum representation $\gamma(\mathbf{q}, \nu)$ and $V_c(\mathbf{q})$ depend only on the momentum transfer \mathbf{q} ,

$$H_{e-ph} = \sum_{\mathbf{q}, \nu, i} \omega_{\mathbf{q}\nu} \hat{n}_i [u_i(\mathbf{q}, \nu) d_{\mathbf{q}\nu} + H.c.], \quad (3)$$

and

$$H_{e-e} = \frac{1}{2} \sum_{i \neq j} V_c(\mathbf{m} - \mathbf{n}) \hat{n}_i \hat{n}_j. \quad (4)$$

Here

$$u_i(\mathbf{q}, \nu) = \frac{1}{\sqrt{2N}} \gamma(\mathbf{q}, \nu) e^{i\mathbf{q}\cdot\mathbf{m}} \quad (5)$$

and

$$V_c(\mathbf{m}) = \frac{1}{N} \sum_{\mathbf{q}} V_c(\mathbf{q}) e^{i\mathbf{q}\cdot\mathbf{m}}, \quad (6)$$

are the matrix elements of e-ph and Coulomb interactions, respectively, in the Wannier representation for electrons, $\hat{n}_i = c_i^\dagger c_i$ is the electron density operator, and $d_{\mathbf{q}\nu}$ annihilates the ν -branch phonon with the wave vector \mathbf{q} and frequency $\omega_{\mathbf{q}\nu}$. Taking the interaction matrix elements depending only on the momentum transfer one neglects terms in the electron-phonon and Coulomb interactions, which are proportional to the overlap integrals of the Wannier orbitals on different sites. This approximation is justified for narrow band materials with the bandwidth $2D$ less than the characteristic value of the crystal field. As a result, the generic Hamiltonian takes the following form in the Wannier representation,

$$\begin{aligned} H = & \sum_{i,j} [T(\mathbf{m} - \mathbf{m}')\delta_{ss'} - \mu\delta_{ij}] c_i^\dagger c_j + \sum_{\mathbf{q}, \nu, i} \omega_{\mathbf{q}\nu} \hat{n}_i [u_i(\mathbf{q}, \nu) d_{\mathbf{q}\nu} + H.c.] \\ & + \frac{1}{2} \sum_{i \neq j} V_c(\mathbf{m} - \mathbf{n}) \hat{n}_i \hat{n}_j + \sum_{\mathbf{q}} \omega_{\mathbf{q}\nu} (d_{\mathbf{q}\nu}^\dagger d_{\mathbf{q}\nu} + 1/2). \end{aligned} \quad (7)$$

Here we confine our discussions to a single electron band and the e-ph matrix element depending only on the momentum transfer \mathbf{q} . This approximation allows for qualitative and in many cases quantitative descriptions of essential polaronic effects in advanced materials. There are might be degenerate atomic orbitals in solids coupled to local molecular-type Jahn-Teller distortions, where one has to consider multi-band electron energy structures (see [42]).

The quantitative calculation of the matrix element in the whole region of momenta has to be performed from pseudopotentials [43, 44, 45]. On the other hand one can parameterize the e-ph interaction rather than to compute it from first principles in many physically important cases [46]. There are three most important interactions in doped semiconductors, which are polar coupling to optical phonons (i.e the Fröhlich e-ph interaction), deformation potential coupling to acoustical phonons, and the local (Holstein) e-ph interaction with molecular type vibrations in complex lattices. While the matrix element is ill defined in metals, it is well defined in doped semiconductors, which have their parent dielectric compounds, together with bare phonons $\omega_{\mathbf{q}\nu}$ and the electron band structure $E_{\mathbf{k}}$. Here the effect of carriers on the crystal field and on the dynamic matrix is small while the carrier density is much less than the atomic one (for phonon self-energies and frequency renormalizations in polaronic systems see Ref. [20, 47]). Hence one can use the band structure and the crystal field of parent insulators to calculate the matrix element in doped semiconductors.

The e-ph matrix element $\gamma(\mathbf{q})$ has different q -dependence for different phonon branches. In the long wavelength limit ($q \ll \pi/a$, a is the lattice constant), $\gamma(\mathbf{q}) \propto q^n$, where $n = -1, 0$ and $n = -1/2$ for polar optical, molecular ($\omega_{\mathbf{q}} = \omega_0$) and acoustic ($\omega_{\mathbf{q}} \propto q$) phonons, respectively. Not only q dependence is known but also the absolute values of $\gamma(\mathbf{q})$ are well parameterized in this limit. For example in polar semiconductors the interaction of two slow electrons at some distance r is found as (see below)

$$v(r) = V_c(r) - \frac{1}{N} \sum_{\mathbf{q}} |\gamma(\mathbf{q})|^2 \omega_{\mathbf{q}} e^{i\mathbf{q}\cdot\mathbf{r}}. \quad (8)$$

The Coulomb repulsion in a rigid lattice is $V_c(r) = e^2/\epsilon_{\infty}r$, and the second term represents the difference between the Coulomb repulsion screened with the core electrons and the repulsion screened with both core electrons and ions. Hence the matrix element of the Fröhlich interaction depends only on the dielectric constants and the optical phonon frequency ω_0 as

$$|\gamma(\mathbf{q})|^2 = \frac{4\pi e^2}{\kappa\omega_0}, \quad (9)$$

where $\kappa = (\epsilon_{\infty}^{-1} - \epsilon_0^{-1})^{-1}$.

One can transform the e-ph interaction further using the site-representation also for phonons. The site representation of phonons is particularly convenient

for the interaction with dispersionless local modes, whose $\omega_{\mathbf{q}\nu} = \omega_\nu$ and the polarization vectors $\mathbf{e}_{\mathbf{q}\nu} = \mathbf{e}_\nu$ are \mathbf{q} independent. Introducing the phonon site-operators

$$d_{\mathbf{n}\nu} = \frac{1}{\sqrt{N}} \sum_{\mathbf{k}} e^{i\mathbf{q}\cdot\mathbf{n}} d_{\mathbf{q}\nu} \quad (10)$$

one transforms the deformation energy and the e-ph interaction as [23]

$$H_{ph} = \sum_{\mathbf{n},\nu} \omega_\nu (d_{\mathbf{n}\nu}^\dagger d_{\mathbf{n}\nu} + 1/2), \quad (11)$$

and

$$H_{e-ph} = \sum_{\mathbf{n},\mathbf{m},\nu} \omega_\nu g_\nu(\mathbf{m} - \mathbf{n}) (\mathbf{e}_\nu \cdot \mathbf{e}_{\mathbf{m}-\mathbf{n}}) \hat{n}_{\mathbf{m}\mathbf{s}} (d_{\mathbf{n}\nu}^\dagger + d_{\mathbf{n}\nu}), \quad (12)$$

respectively.

Here $g_\nu(\mathbf{m})$ is a dimensionless *force* acting between the electron on site \mathbf{m} and the displacement of ion \mathbf{n} , and $\mathbf{e}_{\mathbf{m}-\mathbf{n}} \equiv (\mathbf{m} - \mathbf{n})/|\mathbf{m} - \mathbf{n}|$ is the unit vector in the direction from the electron \mathbf{m} to the ion \mathbf{n} . This real space representation is convenient in modelling the electron-phonon interaction in complex lattices. Atomic orbitals of an ion adiabatically follow its motion. Therefore the electron does not interact with the displacement of the ion, whose orbital it occupies, that is $g_\nu(0) = 0$.

3 Breakdown of Migdal-Eliashberg theory in the strong-coupling regime

Obviously a perturbative approach to the e-ph interaction fails when $\lambda > 1$. However one might expect that the self-consistent Migdal-Eliashberg (ME) theory is still valid in the strong-coupling regime because it sums the infinite set of particular non-crossing diagrams in the electron self-energy. One of the problems with such an extension of the ME theory is a lattice instability. The same theory applied to phonons yields the renormalised phonon frequency $\tilde{\omega} = \omega(1-2\lambda)^{1/2}$ [11]. The frequency turns out to be zero at $\lambda = 0.5$. Because of this lattice instability Migdal [11] and Eliashberg [13] restricted the applicability of their approach to $\lambda < 1$. However, it was shown later that there was no lattice instability, but only a small renormalisation of the phonon frequencies of the order of the adiabatic ratio, $\omega/\mu \ll 1$, for *any* value of λ , if the adiabatic Born-Oppenheimer approach was properly applied [48]. The conclusion was that the Fröhlich Hamiltonian correctly describes the electron self-energy for any value of λ , but it should not be applied to further renormalise phonons.

In fact, ME theory cannot be applied at $\lambda > 1$ for the reason, which has nothing to do with the lattice instability. Actually the $1/\lambda$ multi-polaron expansion technique [20] shows that the many-electron system collapses into the small polaron (or bipolaron) regime at $\lambda \approx 1$ for any adiabatic ratio.

To illustrate the point let us compare the Migdal solution of the simple molecular-chain Holstein model [49] with the exact solution [22] in the adiabatic limit, $\omega_0/t \rightarrow 0$, where $t = T(a)$ is the nearest neighbour hopping integral. The Hamiltonian of the model is

$$H = -t \sum_{\langle ij \rangle} c_i^\dagger c_j + H.c. + 2(\lambda kt)^{1/2} \sum_i x_i c_i^\dagger c_i + \sum_i \left(-\frac{1}{2M} \frac{\partial^2}{\partial x_i^2} + \frac{kx_i^2}{2} \right), \quad (13)$$

where x_i is the normal coordinate of the molecule (site) i , and $k = M\omega^2$. The Migdal theorem is exact in this limit. Hence in the framework of the Migdal-Eliashberg theory one would expect the Fermi-liquid behaviour above T_c and the BCS ground state below T_c at any value of λ . In fact, the exact ground state is a self-trapped insulator at any filling of the band, if $\lambda \geq 1$.

First we consider a two-site case (zero dimensional limit), $i, j = 1, 2$ with one electron, and then generalise the result for an infinite lattice with many electrons. The transformation $X = (x_1 + x_2)$, $\xi = x_1 - x_2$ allows us to eliminate the coordinate X , which is coupled only with the total density ($n_1 + n_2 = 1$). That leaves the following Hamiltonian to be solved in the extreme adiabatic limit $M \rightarrow \infty$:

$$H = -t(c_1^\dagger c_2 + c_2^\dagger c_1) + (\lambda kt)^{1/2} \xi (c_1^\dagger c_1 - c_2^\dagger c_2) + \frac{k\xi^2}{4}. \quad (14)$$

The solution is

$$\psi = (\alpha c_1^\dagger + \beta c_2^\dagger) |0\rangle, \quad (15)$$

where

$$\alpha = \frac{t}{[t^2 + ((\lambda kt)^{1/2} \xi + (t^2 + \lambda kt \xi^2)^{1/2})^2]^{1/2}}, \quad (16)$$

$$\beta = -\frac{(\lambda kt)^{1/2} \xi + (t^2 + \lambda kt \xi^2)^{1/2}}{[t^2 + ((\lambda kt)^{1/2} \xi + (t^2 + \lambda kt \xi^2)^{1/2})^2]^{1/2}}, \quad (17)$$

and the energy is

$$E = \frac{k\xi^2}{4} - (t^2 + \lambda kt \xi^2)^{1/2}. \quad (18)$$

In the extreme adiabatic limit the displacement ξ is classical, so the ground state energy E_0 and the ground state displacement ξ_0 are obtained by minimising Eq.(18) with respect to ξ . If $\lambda \geq 0.5$ we obtain

$$E_0 = -t\left(\lambda + \frac{1}{4\lambda}\right), \quad (19)$$

and

$$\xi_0 = \left[\frac{t(4\lambda^2 - 1)}{\lambda k} \right]^{1/2}. \quad (20)$$

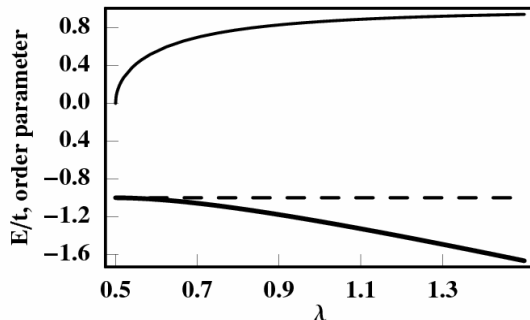


Fig. 1. The ground-state energy (in units of t , solid line) and the order parameter (thin solid line) of the adiabatic Holstein model. The Migdal solution is shown as the dashed line

The symmetry-breaking "order" parameter is

$$\Delta \equiv \beta^2 - \alpha^2 = \frac{[2\lambda + (4\lambda^2 - 1)^{1/2}]^2 - 1}{[2\lambda + (4\lambda^2 - 1)^{1/2}]^2 + 1}. \quad (21)$$

If $\lambda < 0.5$, the ground state is translation invariant, $\Delta = 0$, and $E_0 = -t$, $\xi = 0$, $\beta = -\alpha$. Precisely This state is the "Migdal" solution of the Holstein model, which is symmetric (translation invariant) with $|\alpha| = |\beta|$. When $\lambda < 0.5$, the Migdal solution is the *only* solution. However, when $\lambda > 0.5$ this solution is *not* the ground state of the system, Fig.1. The system collapses into a localised adiabatic polaron trapped on the "right" or on the "left-hand" site due to the finite lattice deformation $\xi_0 \neq 0$.

The generalisation for a multi-polaron system on the infinite lattice of any dimension is straightforward in the extreme adiabatic regime. The adiabatic solution of the infinite one-dimensional (1D) chain with one electron was obtained by Rashba [50] in a continuous (i.e. effective mass) approximation, and by Holstein [49] and Kabanov and Mashtakov [25, 47] for a discrete lattice. The latter authors studied the Holstein two-dimensional (2D) and three-dimensional (3D) lattices in the adiabatic limit. According to Ref. [25] the self-trapping of a single electron occurs at $\lambda \geq 0.875$ and at $\lambda \geq 0.92$ in 2D and 3D, respectively. The radius of the self-trapped adiabatic polaron, r_p , is readily derived from its continuous wave function [50]

$$\psi(r) \sim 1/\cosh(\lambda r/a). \quad (22)$$

It becomes smaller than the lattice constant, $r_p = a/\lambda$ for $\lambda \geq 1$. Hence the multi-polaron system remains in the self-trapped insulating state in the

strong-coupling adiabatic regime, no matter how many polarons it has. The only instability which might occur in this regime is the formation of self-trapped bipolarons, if the on-site attractive interaction, $2\lambda zt$, is larger than the repulsive Hubbard U [51]. Self-trapped on-site bipolarons form a charge ordered state due to a weak repulsion between them [41, 36] (see also [52]).

The transition into the self-trapped state due to a broken translational symmetry is expected at $0.5 < \lambda < 1.3$ (depending on the lattice dimensionality) for any electron-phonon interaction conserving the on-site electron occupation numbers. For example, Hiramoto and Toyozawa [53] calculated the strength of the deformation potential, which transforms electrons into small polarons and bipolarons. They found that the transition of two electrons into a self-trapped small bipolaron occurs at the electron-acoustic phonon coupling $\lambda \simeq 0.5$, that is half of the critical value of λ at which the transition of the electron into the small acoustic polaron takes place in the extreme adiabatic limit, $\omega \ll zt$ (here z is the coordination lattice number). The effect of the adiabatic ratio ω/zt on the critical value of λ was found to be negligible. The radius of the acoustic polaron and bipolaron is about the lattice constant, so that the critical value of λ does not very much depend on the number of electrons in this case either. As discussed below the non-adiabatic corrections (phonons) allow polarons and bipolarons to propagate as the Bloch states in narrow bands.

4 Polaron dynamics

4.1 Polaron band

A self-consistent approach to the multy-polaron problem is possible with the "1/ λ " expansion technique [20], which treats the kinetic energy as a perturbation. The technique is based on the fact, known for a long time, that there is an analytical exact solution of a *single* polaron problem in the strong-coupling limit $\lambda \rightarrow \infty$ [19]. Following Lang and Firsov we apply the canonical transformation e^S to diagonalise the Hamiltonian. The diagonalisation is exact, if $T(\mathbf{m}) = 0$ (or $\lambda = \infty$):

$$\tilde{H} = e^S H e^{-S}, \quad (23)$$

where

$$S = - \sum_{\mathbf{q}, \nu, i} \hat{n}_i [u_i(\mathbf{q}, \nu) d_{\mathbf{q}\nu} - H.c.] \quad (24)$$

is such that $S^\dagger = -S$. The electron and phonon operators are transformed as

$$\tilde{c}_i = c_i \exp \left[\sum_{\mathbf{q}} u_i(\mathbf{q}, \nu) d_{\mathbf{q}\nu} - H.c. \right], \quad (25)$$

and

$$\tilde{d}_{\mathbf{q}\nu} = d_{\mathbf{q}\nu} - \sum_i \hat{n}_i u_i^*(\mathbf{q}, \nu), \quad (26)$$

respectively. It follows from Eq.(27) that the Lang-Firsov canonical transformation shifts the ions to new equilibrium positions. In a more general sense it changes the boson vacuum. As a result, the transformed Hamiltonian takes the following form

$$\tilde{H} = \sum_{i,j} [\hat{\sigma}_{ij} - \mu \delta_{ij}] c_i^\dagger c_j - E_p \sum_i \hat{n}_i + \sum_{\mathbf{q}, \nu} \omega_{\mathbf{q}\nu} (d_{\mathbf{q}\nu}^\dagger d_{\mathbf{q}\nu} + 1/2) + \frac{1}{2} \sum_{i \neq j} v_{ij} \hat{n}_i \hat{n}_j, \quad (27)$$

where

$$\hat{\sigma}_{ij} = T(\mathbf{m} - \mathbf{n}) \delta_{ss'} \exp \left(\sum_{\mathbf{q}, \nu} [u_j(\mathbf{q}, \nu) - u_i(\mathbf{q}, \nu)] d_{\mathbf{q}\nu} - H.c. \right) \quad (28)$$

is the renormalised hopping integral depending on the phonon operators, and

$$v_{ij} \equiv v(\mathbf{m} - \mathbf{n}) = V_c(\mathbf{m} - \mathbf{n}) - \frac{1}{N} \sum_{\mathbf{q}, \nu} |\gamma(\mathbf{q}, \nu)|^2 \omega_{\mathbf{q}\nu} \cos[\mathbf{q} \cdot (\mathbf{m} - \mathbf{n})] \quad (29)$$

is the interaction of polarons comprising their Coulomb repulsion and the interaction via a local lattice deformation. In the extreme infinite-coupling limit, $\lambda \rightarrow \infty$, we can neglect the hopping term of the transformed Hamiltonian. The rest has analytically determined eigenstates and eigenvalues. The eigenstates $|\tilde{N}\rangle = |n_i, n_{\mathbf{q}\nu}\rangle$ are sorted by the polaron $n_{\mathbf{m}s}$ and phonon $n_{\mathbf{q}\nu}$ occupation numbers. The energy levels are

$$E = -(\mu + E_p) \sum_i n_i + \frac{1}{2} \sum_{i \neq j} v_{ij} n_i n_j + \sum_{\mathbf{q}} \omega_{\mathbf{q}\nu} (n_{\mathbf{q}\nu} + 1/2), \quad (30)$$

where $n_i = 0, 1$ and $n_{\mathbf{q}\nu} = 0, 1, 2, 3, \dots, \infty$.

The Hamiltonian, Eq.(27), in zero order with respect to the hopping describes localised polarons and independent phonons, which are vibrations of ions relative to new equilibrium positions depending on the polaron occupation numbers. The phonon frequencies remain unchanged in this limit. The middle of the electron band falls by the polaron level shift E_p due to a potential well created by lattice deformation, Fig.2,

$$E_p = \frac{1}{2N} \sum_{\mathbf{q}, \nu} |\gamma(\mathbf{q}, \nu)|^2 \omega_{\mathbf{q}\nu}. \quad (31)$$

Now let us discuss the $1/\lambda$ expansion. First we restrict the discussion to a single-polaron problem with no polaron-polaron interaction and $\mu = 0$. The finite hopping term leads to the polaron tunnelling because of degeneracy of

the zero order Hamiltonian with respect to the site position of the polaron. To see how the tunnelling occurs we apply the perturbation theory using $1/\lambda$ as a small parameter, where

$$\lambda \equiv \frac{E_p}{D}, \quad (32)$$

and $D = zt$. The proper Bloch set of N -degenerate zero order eigenstates with the lowest energy ($-E_p$) of the unperturbed Hamiltonian is

$$|\mathbf{k}, 0\rangle = \frac{1}{\sqrt{N}} \sum_{\mathbf{m}} c_{\mathbf{m}s}^\dagger \exp(i\mathbf{k} \cdot \mathbf{m})|0\rangle, \quad (33)$$

where $|0\rangle$ is the vacuum. By applying the textbook perturbation theory one readily calculates the perturbed energy levels. Up to the second order in the hopping integral they are given by

$$E(\mathbf{k}) = -E_p + \epsilon_{\mathbf{k}} - \sum_{\mathbf{k}', n_{\mathbf{q}\nu}} \frac{|\langle \mathbf{k}, 0 | \sum_{i,j} \hat{\sigma}_{ij} c_i^\dagger c_j | \mathbf{k}', n_{\mathbf{q}\nu} \rangle|^2}{\sum_{\mathbf{q}, \nu} \omega_{\mathbf{q}\nu} n_{\mathbf{q}\nu}}, \quad (34)$$

where $|\mathbf{k}', n_{\mathbf{q}\nu}\rangle$ are the excited states of the unperturbed Hamiltonian with one electron and at least one real phonon. The second term in Eq.(34), which is linear with respect to the bare hopping $T(\mathbf{m})$, describes the polaron-band dispersion,

$$\epsilon_{\mathbf{k}} = \sum_{\mathbf{m}} T(\mathbf{m}) e^{-g^2(\mathbf{m})} \exp(-i\mathbf{k} \cdot \mathbf{m}), \quad (35)$$

where

$$g^2(\mathbf{m}) = \frac{1}{2N} \sum_{\mathbf{q}, \nu} |\gamma(\mathbf{q}, \nu)|^2 [1 - \cos(\mathbf{q} \cdot \mathbf{m})] \quad (36)$$

is the *band-narrowing factor* at zero temperature. The third term in Eq.(34), quadratic in $T(\mathbf{m})$, yields a negative almost \mathbf{k} -independent correction to the polaron level shift of the order of $1/\lambda^2$. The origin of this correction, which could be much larger than the first-order contribution (Eq.(35) contains a small exponent), is understood in Fig.2. The polaron localised in the potential well of the depth E_p on the site \mathbf{m} , hops onto a neighbouring site \mathbf{n} with no deformation around and comes back. As any second order correction this transition shifts the energy down by an amount of about $-t^2/E_p$. It has little to do with the polaron effective mass and the polaron tunneling mobility because the lattice deformation around \mathbf{m} does not follow the electron. The electron hops back and forth many times (about e^{g^2}) waiting for a sufficient lattice deformation to appear around the site \mathbf{n} . Only after the deformation around \mathbf{n} is created does the polaron tunnel onto the next site together with the deformation.

Oddly enough, analysing the Holstein two-site model some authors took the second-order correction in t in Eq.(34) as a measure of the polaron motion

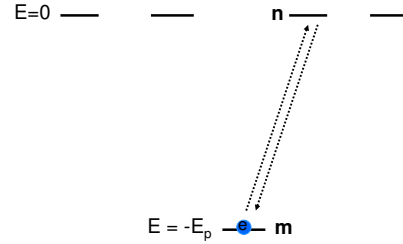


Fig. 2. "Back and forth" virtual transitions of the polaron without any transfer of the lattice deformation from one site to another. These transitions shift the middle of the band further down without any real charge delocalization

and arrived at an erroneous conclusion that "polarons are no longer describable in terms of quasiparticles having a well-defined dispersion" [54] and "the Lang-Firsov approach, which is generally believed to become exact in the limit of antiadiabaticity and an electron-phonon coupling going to infinity, actually diverges most from the exact results precisely in this limit..." [55, 56]. Later on it became clear [57, 58, 59] that this controversy is the result of the erroneous identification of the polaron kinetic energy by the authors of Refs. [54, 55, 56].

4.2 Polaron spectral and Green's functions

The multi-polaron problem has an exact solution in the extreme infinite-coupling limit, $\lambda = \infty$, for any type of e-ph interaction conserving the on-site occupation numbers of electrons. For the finite coupling $1/\lambda$ perturbation expansion is applied. The expansion parameter is actually [9, 60, 61, 20]

$$\frac{1}{2z\lambda^2} \ll 1,$$

so that the analytical perturbation theory has a wider region of applicability than one can expect using a semiclassical estimate $E_p > D$. However, the expansion convergency is different for different e-ph interactions. Exact numerical diagonalisations of vibrating clusters, variational calculations (see Refs. [26, 27, 28, 27, 32, 37, 35] and [62, 63]), dynamical mean-field approach in infinite dimensions [34], and Quantum-Monte-Carlo simulations (see Refs. [64, 38, 65, 66, 67, 68, 69, 70] and [42, 71]) simulations revealed that the

ground state energy ($\approx -E_p$) is not very sensitive to the parameters. On the contrary, the effective mass, the bandwidth, and the polaron density of states strongly depend on the adiabatic ratio ω/t and on the radius of the interaction. The first-order in $1/\lambda$ perturbation theory is practically exact in the non-adiabatic regime $\omega > t$ for any value of the coupling constant and any type of e-ph interaction. However, it *overestimates* the polaron mass by a few orders of magnitude in the adiabatic case, $\omega \ll t$, if the interaction is short-ranged [26].

A much lower effective mass of the adiabatic Holstein polaron compared with that estimated using the first order perturbation theory is the result of poor convergency of the perturbation expansion owing to the double-well potential [49] in the adiabatic limit. The tunnelling probability is extremely sensitive to the shape of this potential and also to the phonon frequency dispersion. The latter leads to a much lighter Holstein polaron compared with the nondispersive approximation [72]. Importantly, the analytical perturbation theory becomes practically exact in a wider range of the adiabatic parameter and of the coupling constant for the long-range Fröhlich interaction [38].

Keeping this in mind, let us calculate the one-particle GF in the first order in $1/\lambda$. Applying the canonical transformation we write the transformed Hamiltonian as

$$\tilde{H} = H_p + H_{ph} + H_{int}, \quad (37)$$

where

$$H_p = \sum_{\mathbf{k}} \xi(\mathbf{k}) c_{\mathbf{k}}^{\dagger} c_{\mathbf{k}} \quad (38)$$

is the “free” *polaron* contribution,

$$H_{ph} = \sum_{\mathbf{q}} \omega_{\mathbf{q}} (d_{\mathbf{q}}^{\dagger} d_{\mathbf{q}} + 1/2) \quad (39)$$

is the free phonon part (spin and phonon branch quantum numbers are dropped here), and $\xi_{\mathbf{k}} = Z' E_{\mathbf{k}} - \mu$ is the renormalised polaron-band dispersion. The chemical potential μ includes the polaron level shift $-E_p$, and it could also include all higher orders in $1/\lambda$ corrections to the polaron spectrum, which are independent of \mathbf{k} . The band-narrowing factor Z' is defined as

$$Z' = \frac{\sum_{\mathbf{m}} T(\mathbf{m}) e^{-g^2(\mathbf{m})} \exp(-i\mathbf{k} \cdot \mathbf{m})}{\sum_{\mathbf{m}} T(\mathbf{m}) \exp(-i\mathbf{k} \cdot \mathbf{m})}, \quad (40)$$

which is $Z' = \exp(-\gamma E_p/\omega)$ with $\gamma \leq 1$ depending on the range of the e-ph interaction and phonon frequency dispersions. The interaction term H_{int} comprises the polaron-polaron interaction, Eq.(29), and the residual polaron-phonon interaction

$$H_{p-ph} \equiv \sum_{i \neq j} [\hat{\sigma}_{ij} - \langle \hat{\sigma}_{ij} \rangle_{ph}] c_i^{\dagger} c_j, \quad (41)$$

where $\langle \hat{\sigma}_{ij} \rangle_{ph}$ means averaging with respect to the bare phonon distribution. We can neglect H_{p-ph} in the first-order of $1/\lambda \ll 1$. To understand spectral properties of a single polaron we also neglect the polaron-polaron interaction. Then the energy levels are

$$E_{\tilde{m}} = \sum_{\mathbf{k}} \xi_{\mathbf{k}} n_{\mathbf{k}} + \sum_{\mathbf{q}} \omega_{\mathbf{q}} [n_{\mathbf{q}} + 1/2], \quad (42)$$

and the transformed eigenstates $|\tilde{m}\rangle$ are sorted by the polaron Bloch-state occupation numbers, $n_{\mathbf{k}} = 0, 1$, and the phonon occupation numbers, $n_{\mathbf{q}} = 0, 1, 2, \dots, \infty$.

The spectral function of any system described by quantum numbers m, n and eigenvalues E_n, E_m is defined as (see, for example [23])

$$A(\mathbf{k}, \omega) \equiv \pi(1 + e^{-\omega/T}) e^{\Omega/T} \sum_{n,m} e^{-E_n/T} |\langle n | c_{\mathbf{k}} | m \rangle|^2 \delta(\omega_{nm} + \omega). \quad (43)$$

It is real and positive, $A(\mathbf{k}, \omega) > 0$, and obeys the important sum rule

$$\frac{1}{\pi} \int_{-\infty}^{\infty} d\omega A(\mathbf{k}, \omega) = 1. \quad (44)$$

Here Ω is the thermodynamic potential. The matrix elements of the electron operators can be written as

$$\langle n | c_{\mathbf{k}} | m \rangle = \frac{1}{\sqrt{N}} \sum_{\mathbf{m}} e^{-i\mathbf{k} \cdot \mathbf{m}} \langle \tilde{n} | c_i \hat{X}_i | \tilde{m} \rangle \quad (45)$$

by the use of the Wannier representation and the Lang-Firsov transformation. Here

$$\hat{X}_i = \exp \left[\sum_{\mathbf{q}} u_i(\mathbf{q}) d_{\mathbf{q}} - H.c. \right].$$

Now, applying the Fourier transform of the δ -function in Eq.(43),

$$\delta(\omega_{nm} + \omega) = \frac{1}{2\pi} \int_{-\infty}^{\infty} dt e^{i(\omega_{nm} + \omega)t},$$

the spectral function is expressed as

$$A(\mathbf{k}, \omega) = \frac{1}{2} \int_{-\infty}^{\infty} dt e^{i\omega t} \frac{1}{N} \sum_{\mathbf{m}, \mathbf{n}} e^{i\mathbf{k} \cdot (\mathbf{n} - \mathbf{m})} \times \quad (46)$$

$$\left\{ \left\langle \left\langle c_i(t) \hat{X}_i(t) c_j^\dagger \hat{X}_j^\dagger \right\rangle \right\rangle + \left\langle \left\langle c_j^\dagger \hat{X}_j^\dagger c_i(t) \hat{X}_i(t) \right\rangle \right\rangle \right\}.$$

Here the quantum and statistical averages are performed for independent polarons and phonons, therefore

$$\langle\langle c_i(t)\hat{X}_i(t)\hat{X}_j^\dagger c_i^\dagger \rangle\rangle = \langle\langle c_i(t)c_j^\dagger \rangle\rangle \langle\langle \hat{X}_i(t)\hat{X}_j^\dagger \rangle\rangle. \quad (47)$$

The Heisenberg free-polaron operator evolves with time as

$$c_{\mathbf{k}}(t) = c_{\mathbf{k}}e^{-i\xi_{\mathbf{k}}t}, \quad (48)$$

and

$$\begin{aligned} \langle\langle c_i(t)c_i^\dagger \rangle\rangle &= \frac{1}{N} \sum_{\mathbf{k}', \mathbf{k}''} e^{i(\mathbf{k}' \cdot \mathbf{m} - \mathbf{k}'' \cdot \mathbf{n})} \langle\langle c_{\mathbf{k}'}(t)c_{\mathbf{k}''}^\dagger \rangle\rangle = \\ &= \frac{1}{N} \sum_{\mathbf{k}'} [1 - \bar{n}(\mathbf{k}')] e^{i\mathbf{k}' \cdot (\mathbf{m} - \mathbf{n}) - i\xi_{\mathbf{k}'}t}, \end{aligned} \quad (49)$$

$$\langle\langle c_i^\dagger c_i(t) \rangle\rangle = \frac{1}{N} \sum_{\mathbf{k}'} \bar{n}(\mathbf{k}') e^{i\mathbf{k}' \cdot (\mathbf{m} - \mathbf{n}) - i\xi_{\mathbf{k}'}t} \quad (50)$$

where $\bar{n}(\mathbf{k}) = [1 + \exp \xi_{\mathbf{k}}/T]^{-1}$ is the Fermi-Dirac distribution function of polarons. The Heisenberg free-phonon operator evolves in a similar way,

$$d_{\mathbf{q}}(t) = d_{\mathbf{q}}e^{-i\omega_{\mathbf{q}}t},$$

and

$$\langle\langle \hat{X}_i(t)\hat{X}_j^\dagger \rangle\rangle = \prod_{\mathbf{q}} \langle\langle \exp[u_i(\mathbf{q},t)d_{\mathbf{q}} - H.c.] \exp[-u_j(\mathbf{q})d_{\mathbf{q}} - H.c.] \rangle\rangle, \quad (51)$$

where $u_{i,j}(\mathbf{q},t) = u_{i,j}(\mathbf{q})e^{-i\omega_{\mathbf{q}}t}$. This average is calculated using the operator identity

$$e^{\hat{A}+\hat{B}} = e^{\hat{A}}e^{\hat{B}}e^{-[\hat{A},\hat{B}]/2}, \quad (52)$$

which is applied for any two operators \hat{A} and \hat{B} , whose commutator $[\hat{A}, \hat{B}]$ is a number. Because $[d_{\mathbf{q}}, d_{\mathbf{q}}^\dagger] = 1$, we can apply this identity in Eq.(51) to obtain

$$e^{[u_i(\mathbf{q},t)d_{\mathbf{q}} - H.c.]} e^{[-u_j(\mathbf{q})d_{\mathbf{q}} - H.c.]} = e^{(\alpha^* d_{\mathbf{q}}^\dagger - \alpha d_{\mathbf{q}})} \times e^{[u_i(\mathbf{q},t)u_j^*(\mathbf{q}) - u_i^*(\mathbf{q},t)u_j(\mathbf{q})]/2},$$

where $\alpha \equiv u_j(\mathbf{q},t) - u_i(\mathbf{q})$. Applying once again the same identity yields

$$e^{[u_i(\mathbf{q},t)d_{\mathbf{q}} - H.c.]} e^{[-u_j(\mathbf{q})d_{\mathbf{q}} - H.c.]} = e^{\alpha^* d_{\mathbf{q}}^\dagger} e^{-\alpha d_{\mathbf{q}}} e^{-|\alpha|^2/2} \times e^{[u_i(\mathbf{q},t)u_j^*(\mathbf{q}) - u_i^*(\mathbf{q},t)u_j(\mathbf{q})]/2}. \quad (53)$$

Now the quantum and statistical averages are calculated by the use of

$$\langle\langle e^{\alpha^* d_{\mathbf{q}}^\dagger} e^{-\alpha d_{\mathbf{q}}} \rangle\rangle = e^{-|\alpha|^2 n_\omega}, \quad (54)$$

where $n_\omega = [\exp(\omega_{\mathbf{q}}/T) - 1]^{-1}$ is the Bose-Einstein distribution function of phonons. Collecting all multiplies in Eq.(51) we arrive at

$$\langle\langle \hat{X}_i(t)\hat{X}_j^\dagger \rangle\rangle = \exp\left\{-\frac{1}{2N}\sum_{\mathbf{q}}|\gamma(\mathbf{q})|^2 f_{\mathbf{q}}(\mathbf{m}-\mathbf{n},t)\right\}, \quad (55)$$

where

$$f_{\mathbf{q}}(\mathbf{m},t) = [1 - \cos(\mathbf{q}\cdot\mathbf{m})\cos(\omega_{\mathbf{q}}t)] \coth\frac{\omega_{\mathbf{q}}}{2T} + i\cos(\mathbf{q}\cdot\mathbf{m})\sin(\omega_{\mathbf{q}}t). \quad (56)$$

Here we used the symmetry of $\gamma(-\mathbf{q}) = \gamma(\mathbf{q})$, because of which terms containing $\sin(\mathbf{q}\cdot\mathbf{m})$ disappeared. The average $\langle\langle \hat{X}_j^\dagger \hat{X}_i(t) \rangle\rangle$, which is a multiplier in the second term in the brackets of Eq.(46), is obtained as

$$\langle\langle \hat{X}_j^\dagger \hat{X}_i(t) \rangle\rangle = \langle\langle \hat{X}_i(t)\hat{X}_j^\dagger \rangle\rangle^*. \quad (57)$$

To proceed with the analytical results we consider low temperatures, $T \ll \omega_{\mathbf{q}}$, when $\coth(\omega_{\mathbf{q}}/2T) \approx 1$. Then expanding the exponent in Eq.(55) yields

$$\langle\langle \hat{X}_i(t)\hat{X}_j^\dagger \rangle\rangle = Z \sum_{l=0}^{\infty} \frac{\left\{\sum_{\mathbf{q}}|\gamma(\mathbf{q})|^2 e^{i[\mathbf{q}\cdot(\mathbf{m}-\mathbf{n})-\omega_{\mathbf{q}}t]}\right\}^l}{(2N)^l l!}, \quad (58)$$

where

$$Z = \exp\left[-\frac{1}{2N}\sum_{\mathbf{q}}|\gamma(\mathbf{q})|^2\right]. \quad (59)$$

Then performing summation over $\mathbf{m}, \mathbf{n}, \mathbf{k}'$ and integration over time in Eq.(46) we arrive at [73]

$$A(\mathbf{k},\omega) = \sum_{l=0}^{\infty} \left[A_l^{(-)}(\mathbf{k},\omega) + A_l^{(+)}(\mathbf{k},\omega) \right], \quad (60)$$

where

$$A_l^{(-)}(\mathbf{k},\omega) = \pi Z \sum_{\mathbf{q}_1, \dots, \mathbf{q}_l} \frac{\prod_{r=1}^l |\gamma(\mathbf{q}_r)|^2}{(2N)^l l!} \times \left[1 - \bar{n} \left(\mathbf{k} - \sum_{r=1}^l \mathbf{q}_r \right) \right] \delta \left(\omega - \sum_{r=1}^l \omega_{\mathbf{q}_r} - \xi_{\mathbf{k} - \sum_{r=1}^l \mathbf{q}_r} \right), \quad (61)$$

and

$$A_l^{(+)}(\mathbf{k},\omega) = \pi Z \sum_{\mathbf{q}_1, \dots, \mathbf{q}_l} \frac{\prod_{r=1}^l |\gamma(\mathbf{q}_r)|^2}{(2N)^l l!} \times \bar{n} \left(\mathbf{k} + \sum_{r=1}^l \mathbf{q}_r \right) \delta \left(\omega + \sum_{r=1}^l \omega_{\mathbf{q}_r} - \xi_{\mathbf{k} + \sum_{r=1}^l \mathbf{q}_r} \right). \quad (62)$$

Clearly Eq.(60) is in the form of a perturbative multi-phonon expansion. Each contribution $A_l^{(\pm)}(\mathbf{k}, \omega)$ to the spectral function describes the transition from the initial state \mathbf{k} of the polaron band to the final state $\mathbf{k} \pm \sum_{r=1}^l \mathbf{q}_r$ with the emission (or absorption) of l phonons.

The $1/\lambda$ expansion result, Eq.(60), is applied to *low-energy* polaron excitations in the strong-coupling limit. In the case of the long-range Fröhlich interaction with high-frequency phonons it is also applied in the intermediate regime [38, 69]. Different from the conventional ME spectral function there is no imaginary part of the self-energy since the exponentially small at low temperatures polaronic damping [23] is neglected. Instead the e-ph coupling leads to the coherent dressing of electrons by phonons. The dressing can be seen as the phonon "side-bands" with $l \geq 1$.

While the major sum rule, Eq.(44) is satisfied,

$$\frac{1}{\pi} \int_{-\infty}^{\infty} d\omega A(\mathbf{k}, \omega) = Z \sum_{l=0}^{\infty} \sum_{\mathbf{q}_1, \dots, \mathbf{q}_l} \frac{\prod_{r=1}^l |\gamma(\mathbf{q}_r)|^2}{(2N)^l l!} = \quad (63)$$

$$Z \sum_{l=0}^{\infty} \frac{1}{l!} \left\{ \frac{1}{2N} \sum_{\mathbf{q}} |\gamma(\mathbf{q})|^2 \right\}^l = Z \exp \left[\frac{1}{2N} \sum_{\mathbf{q}} |\gamma(\mathbf{q})|^2 \right] = 1,$$

the higher-momentum integrals, $\int_{-\infty}^{\infty} d\omega \omega^p A(\mathbf{k}, \omega)$ with $p > 0$, calculated using Eq.(60), differ from the exact values (see Part III) by an amount proportional to $1/\lambda$. The difference is due to a partial "undressing" of high-energy excitations in the side-bands, which is beyond the first order $1/\lambda$ expansion.

The spectral function of the polaronic carriers comprises two different parts. The first ($l = 0$) \mathbf{k} -dependent *coherent* term arises from the polaron band tunnelling,

$$A_{coh}(\mathbf{k}, \omega) = \left[A_0^{(-)}(\mathbf{k}, \omega) + A_0^{(+)}(\mathbf{k}, \omega) \right] = \pi Z \delta(\omega - \xi_{\mathbf{k}}). \quad (64)$$

The spectral weight of the coherent part is suppressed as $Z \ll 1$. However in the case of the Fröhlich interaction the effective mass is less enhanced, $\xi_{\mathbf{k}} = Z' E_{\mathbf{k}} - \mu$, because $Z \ll Z' < 1$.

The second *incoherent* part $A_{incoh}(\mathbf{k}, \omega)$ comprises all the terms with $l \geq 1$. It describes the excitations accompanied by emission and absorption of phonons. We notice that its spectral density spreads over a wide energy range of about twice the polaron level shift E_p , which might be larger than the unrenormalised bandwidth $2D$ in the rigid lattice without phonons. On the contrary, the coherent part shows a dispersion only in the energy window of the order of the polaron bandwidth, $w = Z'D$. It is interesting that there is some \mathbf{k} dependence of the *incoherent* background as well [73], if the matrix element of the e-ph interaction and/or phonon frequencies depend on \mathbf{q} . Only in the Holstein model with the short-range dispersionless e-ph interaction $\gamma(\mathbf{q}) = \gamma_0$ and $\omega_{\mathbf{q}} = \omega_0$ the incoherent part is momentum independent (see also Ref. [46]),

$$A_{incoh}(\mathbf{k}, \omega) = \pi \frac{Z}{N} \sum_{l=1}^{\infty} \frac{\gamma_0^{2l}}{2^l l!} \times \sum_{\mathbf{k}'} \{ [1 - \bar{n}(\mathbf{k}')] \delta(\omega - l\omega_0 - \xi_{\mathbf{k}'}) + \bar{n}(\mathbf{k}') \delta(\omega + l\omega_0 - \xi_{\mathbf{k}'}) \}. \quad (65)$$

As soon as we know the spectral function, different Green's functions (GF) are readily obtained using their analytical properties. Inexpolaron! Green's function For example, the temperature GF is given by the integral [23]

$$\mathcal{G}(\mathbf{k}, \omega_k) = \frac{1}{\pi} \int_{-\infty}^{\infty} d\omega' \frac{A(\mathbf{k}, \omega')}{i\omega_k - \omega'}. \quad (66)$$

where $\omega_k = \pi T(2k + 1)$, $k = 0, \pm 1, \pm 2, \dots$. Calculating the integral with the spectral density Eq.(65) we find in the Holstein model [74]

$$\mathcal{G}(\mathbf{k}, \omega_n) = \frac{Z}{i\omega_n - \xi_{\mathbf{k}}} + \frac{Z}{N} \sum_{l=1}^{\infty} \frac{\gamma_0^{2l}}{2^l l!} \sum_{\mathbf{k}'} \left\{ \frac{1 - \bar{n}(\mathbf{k}')}{i\omega_n - l\omega_0 - \xi_{\mathbf{k}'}} + \frac{\bar{n}(\mathbf{k}')}{i\omega_n + l\omega_0 - \xi_{\mathbf{k}'}} \right\}. \quad (67)$$

Here the first term describes the coherent tunnelling in the narrow polaron band while the second \mathbf{k} -independent sum describes the phonon-side bands.

5 Polaron-polaron interaction and small bipolaron

Polarons interact with each other, Eq.(29). The range of the deformation surrounding the Fröhlich polarons is quite large, and their deformation fields are overlapped at finite density. Taking into account both the long-range attraction of polarons owing to the lattice deformations *and* their direct Coulomb repulsion, the residual *long-range* interaction turns out rather weak and repulsive in ionic crystals [1]. The Fourier component of the polaron-polaron interaction, $v(\mathbf{q})$, comprising the direct Coulomb repulsion and the attraction mediated by phonons is

$$v(\mathbf{q}) = \frac{4\pi e^2}{\epsilon_{\infty} q^2} - |\gamma(\mathbf{q})|^2 \omega_{\mathbf{q}}. \quad (68)$$

In the long-wave limit ($q \ll \pi/a$) the Fröhlich interaction [75] dominates in the attractive part, which is described by Eq.(9). Fourier transforming Eq.(68) yields the repulsive interaction in real space,

$$v(\mathbf{m} - \mathbf{n}) = \frac{e^2}{\epsilon_0 |\mathbf{m} - \mathbf{n}|} > 0. \quad (69)$$

We see that optical phonons nearly nullify the bare Coulomb repulsion in ionic solids, where $\epsilon_0 \gg 1$, but cannot overscreen it at large distances.

Considering the polaron-phonon interaction in the multi-polaron system we have to take into account dynamic properties of the polaron response function [59]. One may erroneously believe that the long-range Fröhlich interaction becomes a short-range (Holstein) one due to the screening of ions by heavy polaronic carriers. In fact, small polarons cannot screen high-frequency optical vibrations because their renormalised plasma frequency is comparable with or even less than the phonon frequency. In the absence of bipolarons (see below) we can apply the ordinary bubble approximation to calculate the dielectric response function of polarons at the frequency Ω as

$$\epsilon(\mathbf{q}, \Omega) = 1 - 2v(\mathbf{q}) \sum_{\mathbf{k}} \frac{\bar{n}(\mathbf{k} + \mathbf{q}) - \bar{n}(\mathbf{k})}{\Omega - \epsilon_{\mathbf{k}} + \epsilon_{\mathbf{k}+\mathbf{q}}}. \quad (70)$$

This expression describes the response of small polarons to any external field of the frequency $\Omega \leq \omega_0$, when phonons in the polaron cloud follow the polaron motion. In the static limit we obtain the usual Debye screening at large distances ($q \rightarrow 0$). For the temperature larger than the polaron half-bandwidth, $T > w$, we can approximate the polaron distribution function as

$$\bar{n}(\mathbf{k}) \approx \frac{n}{2a^3} \left(1 - \frac{(2-n)\epsilon_{\mathbf{k}}}{2T} \right), \quad (71)$$

and obtain

$$\epsilon(q, 0) = 1 + \frac{q_s^2}{q^2}, \quad (72)$$

where

$$q_s = \left[\frac{2\pi e^2 n(2-n)}{\epsilon_0 T a^3} \right]^{1/2},$$

and n is the number of polarons per unit cell. For a finite but rather low frequency, $\omega_0 > \Omega \gg w$, the polaron response becomes dynamic,

$$\epsilon(\mathbf{q}, \Omega) = 1 - \frac{\omega_p^2(\mathbf{q})}{\Omega^2} \quad (73)$$

where

$$\omega_p^2(\mathbf{q}) = 2v(\mathbf{q}) \sum_{\mathbf{k}} n(\mathbf{k})(\epsilon_{\mathbf{k}+\mathbf{q}} - \epsilon_{\mathbf{k}}) \quad (74)$$

is the temperature-dependent polaron plasma frequency squared. The polaron plasma frequency is rather low due to the large static dielectric constant, $\epsilon_0 \gg 1$, and the enhanced polaron mass $m^* \gg m_e$.

Now replacing the bare electron-phonon interaction vertex $\gamma(\mathbf{q})$ by a screened one, $\gamma_{sc}(\mathbf{q}, \omega_0)$, as shown in Fig. 3, we obtain

$$\gamma_{sc}(\mathbf{q}, \omega_0) = \frac{\gamma(\mathbf{q})}{\epsilon(\mathbf{q}, \omega_0)} \approx \gamma(\mathbf{q}) \quad (75)$$

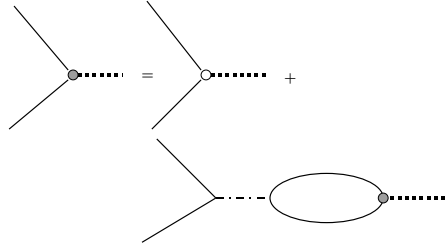


Fig. 3. E-ph vertex, $\gamma(\mathbf{q})$ screened by the polaron-polaron interaction, $v(\mathbf{q})$ (dashed-dotted line). Solid and dotted lines are polaron and phonon propagators, respectively.

because $\omega_0 > \omega_p$. Therefore, the singular behaviour of $\gamma(\mathbf{q}) \sim 1/q$ is unaffected by screening. Polarons are too slow to screen high-frequency crystal field oscillations. As a result, the strong interaction with high-frequency optical phonons in ionic solids remains unscreened at any density of small polarons.

Another important point is a possibility of the Wigner crystallization of the polaronic liquid. Because the net long-range repulsion is relatively weak, a relevant dimensionless parameter $r_s = m^* e^2 / \epsilon_0 (4\pi n / 3)^{1/3}$ is not very large in ionic semiconductors. The Wigner crystallization appears around $r_s \simeq 100$ or larger, which corresponds to the atomic density of polarons $n \leq 10^{-6}$ with $\epsilon_0 = 30$ and $m^* = 5m_e$. This estimate tells us that polaronic carriers are usually in the liquid state at relevant doping levels.

At large distances polarons repel each other. Nevertheless two *large* polarons can be bound into a *large* bipolaron by an exchange interaction even with no additional e-ph interaction but the Fröhlich one [76, 2, 114]. When a short-range deformation potential and molecular-type (i.e. Holstein) e-ph interactions are taken into account together with the Fröhlich interaction, they overcome the Coulomb repulsion at a short distance of about the lattice constant. Then, owing to a narrow band, two small polarons easily form a bound state, i.e. a *small* bipolaron. Let us estimate the coupling constant λ and the adiabatic ratio ω_0/t , at which the "bipolaronic" instability occurs. The characteristic attractive potential is $|v| = D/(\lambda - \mu_c)$, where μ_c is the dimensionless Coulomb repulsion, and λ includes the interaction with all phonon branches. The radius of the potential is about a . In three dimensions a bound state of two attractive particles appears, if

$$|v| \geq \frac{\pi^2}{8m^*a^2}. \quad (76)$$

Substituting the polaron mass, $m^* = [2a^2t]^{-1} \exp(\gamma\lambda D/\omega_0)$, we find

$$\frac{t}{\omega_0} \leq (\gamma z \lambda)^{-1} \ln \left[\frac{\pi^2}{4z(\lambda - \mu_c)} \right]. \quad (77)$$

As a result, small bipolarons form at $\lambda \geq \mu_c + \pi^2/4z$ almost independent of the adiabatic ratio. In the case of the Fröhlich interaction there is no sharp transition between small and large polarons, and the first-order $1/\lambda$ expansion is accurate in the whole region of the e-ph coupling, if the adiabatic parameter is not too small. Hence we can say that in the antiadiabatic and intermediate regime the carriers are small polarons *independent* of the value of λ if the e-ph interaction is long-ranged. It means that they tunnel together with the entire phonon cloud no matter how "thin" the cloud is.

6 Polaronic superconductivity

The polaron-polaron interaction is the sum of two large contributions of the opposite sign, Eq.(29). It is generally larger than the polaron bandwidth and the polaron Fermi-energy, $\epsilon_F = Z' E_F$. This condition is opposite to the weak-coupling BCS regime, where the Fermi energy is the largest. However, there is still a narrow window of parameters, where bipolarons are extended enough, and pairs of two small polarons are overlapped similar to the Cooper pairs. Here the BCS approach is applied to nonadiabatic carriers with a *nonretarded* attraction, so that bipolarons are the Cooper pairs formed by two *small polarons* [18]. The size of the bipolaron is estimated as

$$r_b \approx \frac{1}{(m^* \Delta)^{1/2}}, \quad (78)$$

where Δ is the binding energy of the order of an attraction potential v . The BCS approach is applied if $r_b \gg n^{-1/3}$, which puts a severe constraint on the value of the attraction

$$|v| \ll \epsilon_F. \quad (79)$$

There is no "Tolmachev" logarithm in the case of nonadiabatic carriers, because the attraction is nonretarded as soon as $\epsilon_F \leq \omega_0$. Hence a superconducting state of small polarons is possible only if $\lambda > \mu_c$. This consideration leaves a rather narrow *crossover* region from the normal polaron Fermi liquid to a superconductor, where one can still apply the BCS mean-field approach,

$$0 < \lambda - \mu_c \ll Z' < 1. \quad (80)$$

In the case of the Fröhlich interaction Z' is about $0.1 \div 0.3$ for typical values of λ . Hence the region, Eq.(80), is on the border-line from the polaronic normal metal to a bipolaronic superconductor (section 8).

In the crossover region polarons behave like fermions in a narrow band with a weak nonretarded attraction. As long as $\lambda \gg 1/\sqrt{2z}$, we can neglect their residual interaction with phonons in the transformed Hamiltonian,

$$\tilde{H} \approx \sum_{i,j} \left[(\langle \hat{\sigma}_{ij} \rangle_{ph} - \mu \delta_{ij}) c_i^\dagger c_j + \frac{1}{2} v_{ij} c_i^\dagger c_j^\dagger c_j c_i \right] \quad (81)$$

written in the Wannier representation. If the condition Eq.(80) is satisfied, we can treat the polaron-polaron interaction approximately by the use of the BCS theory. For simplicity let us keep only the on-site v_0 and the nearest-neighbour v_1 interactions. At least one of them should be attractive to ensure that the ground state is superconducting. Introducing two order parameters

$$\Delta_0 = -v_0 \langle c_{\mathbf{m},\uparrow} c_{\mathbf{m},\downarrow} \rangle, \quad (82)$$

$$\Delta_1 = -v_1 \langle c_{\mathbf{m},\uparrow} c_{\mathbf{m}+\mathbf{a},\downarrow} \rangle \quad (83)$$

and transforming to the \mathbf{k} -space results in the familiar BCS Hamiltonian,

$$H_p = \sum_{\mathbf{k},s} \xi_{\mathbf{k}} c_{\mathbf{k}s}^\dagger c_{\mathbf{k}s} + \sum_{\mathbf{k}} [\Delta_{\mathbf{k}} c_{\mathbf{k}\uparrow}^\dagger c_{-\mathbf{k}\downarrow}^\dagger + H.c.], \quad (84)$$

where $\xi_{\mathbf{k}} = \epsilon_{\mathbf{k}} - \mu$ is the renormalised kinetic energy and

$$\Delta_{\mathbf{k}} = \Delta_0 - \Delta_1 \frac{\xi_{\mathbf{k}} + \mu}{w} \quad (85)$$

is the order parameter.

The Bogoliubov anomalous averages are found as

$$\langle c_{\mathbf{k},\uparrow} c_{-\mathbf{k},\downarrow} \rangle = \frac{\Delta_{\mathbf{k}}}{2\sqrt{\xi_{\mathbf{k}}^2 + \Delta_{\mathbf{k}}^2}} \tanh \frac{\sqrt{\xi_{\mathbf{k}}^2 + \Delta_{\mathbf{k}}^2}}{2T}, \quad (86)$$

and two coupled equations for the on-site and inter-site order parameters are

$$\Delta_0 = -\frac{v_0}{N} \sum_{\mathbf{k}} \frac{\Delta_{\mathbf{k}}}{2\sqrt{\xi_{\mathbf{k}}^2 + \Delta_{\mathbf{k}}^2}} \tanh \frac{\sqrt{\xi_{\mathbf{k}}^2 + \Delta_{\mathbf{k}}^2}}{2T}, \quad (87)$$

$$\Delta_1 = -\frac{v_1}{Nw} \sum_{\mathbf{k}} \frac{\Delta_{\mathbf{k}}(\xi_{\mathbf{k}} + \mu)}{2\sqrt{\xi_{\mathbf{k}}^2 + \Delta_{\mathbf{k}}^2}} \tanh \frac{\sqrt{\xi_{\mathbf{k}}^2 + \Delta_{\mathbf{k}}^2}}{2T}. \quad (88)$$

These equations are equivalent to a single BCS equation for $\Delta_{\mathbf{k}} = \Delta(\xi_{\mathbf{k}})$, but with the half polaron bandwidth w cutting the integral, rather than the Debye temperature,

$$\Delta(\xi) = \int_{-w-\mu}^{w-\mu} d\eta N_p(\eta) V(\xi, \eta) \frac{\Delta(\eta)}{2\sqrt{\eta^2 + \Delta(\eta)^2}} \tanh \frac{\sqrt{\eta^2 + \Delta(\eta)^2}}{2T}. \quad (89)$$

Here $V(\xi, \eta) = -v_0 - zv_1(\xi + \mu)(\eta + \mu)/w^2$.

The critical temperature T_c of the polaronic superconductor is determined by two linearised equations in the limit $\Delta_{0,1} \rightarrow 0$,

$$\left[1 + A \left(\frac{v_0}{zv_1} + \frac{\mu^2}{w^2}\right)\right] \Delta - \frac{B\mu}{w} \Delta_1 = 0, \quad (90)$$

$$- \frac{A\mu}{w} \Delta + (1 + B) \Delta_1 = 0, \quad (91)$$

where $\Delta = \Delta_0 - \Delta_1\mu/w$, and

$$A = \frac{zv_1}{2w} \int_{-w-\mu}^{w-\mu} d\eta \frac{\tanh \frac{\eta}{2T_c}}{\eta},$$

$$B = \frac{zv_1}{2w} \int_{-w-\mu}^{w-\mu} d\eta \frac{\eta \tanh \frac{\eta}{2T_c}}{w^2}.$$

These equations are applied only if the polaron-polaron coupling is weak, $|v_{0,1}| < w$. A nontrivial solution is found at

$$T_c \approx 1.14w \sqrt{1 - \frac{\mu^2}{w^2}} \exp\left(\frac{2w}{v_0 + zv_1\mu^2/w^2}\right), \quad (92)$$

if $v_0 + zv_1\mu^2/w^2 < 0$, so that superconductivity exists even in the case of the on-site repulsion, $v_0 > 0$, if this repulsion is less than the total intersite attraction, $z|v_1|$. There is a nontrivial dependence of T_c on doping. With a constant density of states in the polaron band, the Fermi energy $\epsilon_F \approx \mu$ is expressed via the number of polarons per atom n as

$$\mu = w(n - 1), \quad (93)$$

so that

$$T_c \simeq 1.14w \sqrt{n(2-n)} \exp\left(\frac{2w}{v_0 + zv_1[n-1]^2}\right), \quad (94)$$

which has two maxima as a function of n separated by a deep minimum in the half-filled band ($n = 1$), where the nearest-neighbour contributions to pairing are canceled.

7 Mobile small bipolarons

The attractive energy of two small polarons is generally larger than the polaron bandwidth, $\lambda - \mu_c \gg Z'$. When this condition is satisfied, small bipolarons are not overlapped. Consideration of particular lattice structures shows that small bipolarons are mobile even when the electron-phonon coupling is strong and the bipolaron binding energy is large [40, 70]. Here we encounter a novel electronic state of matter, a charged Bose liquid, qualitatively different from the normal Fermi-liquid and the BCS superfluid. The Bose-liquid is stable because bipolarons repel each other (see below).

7.1 On-site bipolarons and bipolaronic Hamiltonian

The small parameter, $Z'/(\lambda - \mu_c) \ll 1$, allows for a consistent treatment of bipolaronic systems [18, 41]. Under this condition the hopping term in the transformed Hamiltonian \tilde{H} is a small perturbation of the ground state of immobile bipolarons and free phonons,

$$\tilde{H} = H_0 + H_{pert}, \quad (95)$$

where

$$H_0 = \frac{1}{2} \sum_{i,j} v_{ij} c_i^\dagger c_j^\dagger c_j c_i + \sum_{\mathbf{q},\nu} \omega_{\mathbf{q}\nu} [d_{\mathbf{q}\nu}^\dagger d_{\mathbf{q}\nu} + 1/2] \quad (96)$$

and

$$H_{pert} = \sum_{i,j} \hat{\sigma}_{ij} c_i^\dagger c_j \quad (97)$$

Let us first discuss the dynamics of *onsite* bipolarons, which are the ground state of the system with the Holstein non-dispersive e-ph interaction [51, 41]. The onsite bipolaron is formed if

$$2E_p > U, \quad (98)$$

where U is the onsite Coulomb correlation energy (the Hubbard U). The intersite polaron-polaron interaction is just the Coulomb repulsion since the phonon mediated attraction between two polarons on different sites is zero in the Holstein model. Two or more onsite bipolarons as well as three or more polarons cannot occupy the same site because of the Pauli exclusion principle. Hence, bipolarons repel single polarons and each other. Their binding energy, $\Delta = 2E_p - U$, is larger than the polaron half-bandwidth, $\Delta \gg w$, so that there are no unbound polarons in the ground state. H_{pert} , Eq.(97), destroys bipolarons in the first order. Hence it has no diagonal matrix elements. Then the bipolaron dynamics, including superconductivity, is described by the use of a new canonical transformation $\exp(S_2)$ [41], which eliminates the first order of H_{pert} ,

$$(S_2)_{fp} = \sum_{i,j} \frac{\langle f | \hat{\sigma}_{ij} c_i^\dagger c_j | p \rangle}{E_f - E_p}. \quad (99)$$

Here $E_{f,p}$ and $|f\rangle, |p\rangle$ are the energy levels and the eigenstates of H_0 . Neglecting the terms of the order higher than $(w/\Delta)^2$ we obtain

$$(H_b)_{ff'} \equiv \left(e^{S_2} \tilde{H} e^{-S_2} \right)_{ff'}, \quad (100)$$

$$(H_b)_{ff'} \approx (H_0)_{ff'} - \frac{1}{2} \sum_{\nu} \sum_{i \neq i', j \neq j'} \langle f | \hat{\sigma}_{i\nu} c_i^\dagger c_{i'} | p \rangle \langle p | \hat{\sigma}_{j\nu} c_j^\dagger c_{j'} | f' \rangle \times \left(\frac{1}{E_p - E_{f'}} + \frac{1}{E_p - E_f} \right).$$

S_2 couples a localised onsite bipolaron and a state of two unbound polarons on different sites. The expression (100) determines the matrix elements of the transformed *bipolaronic* Hamiltonian H_b in the subspace $|f\rangle, |f'\rangle$ with no single (unbound) polarons. On the other hand, the intermediate *bra* $\langle p|$ and *ket* $|p\rangle$ refer to configurations involving two unpaired polarons and any number of phonons. Hence we have

$$E_p - E_f = \Delta + \sum_{\mathbf{q}, \nu} \omega_{\mathbf{q}\nu} (n_{\mathbf{q}\nu}^p - n_{\mathbf{q}\nu}^f), \quad (101)$$

where $n_{\mathbf{q}\nu}^{f,p}$ are phonon occupation numbers $(0, 1, 2, 3, \dots, \infty)$. This equation is an explicit definition of the bipolaron binding energy Δ which takes into account the residual inter-site repulsion between bipolarons and between two unpaired polarons. The lowest eigenstates of H_b are in the subspace, which has only doubly occupied $c_{\mathbf{m}s}^\dagger c_{\mathbf{m}s'}^\dagger |0\rangle$ or empty $|0\rangle$ sites. On-site bipolaron tunnelling is a two-step transition. It takes place via a single polaron tunneling to a neighbouring site. The subsequent tunnelling of its "partner" to the same site restores the initial energy state of the system. There are no *real* phonons emitted or absorbed because the (bi)polaron band is narrow. Hence we can average H_b with respect to phonons. Replacing the energy denominators in the second term in Eq.(100) by the integrals with respect to time,

$$\frac{1}{E_p - E_f} = i \int_0^\infty dt e^{i(E_f - E_p + i\delta)t},$$

we obtain

$$H_b = H_0 - i \sum_{\mathbf{m} \neq \mathbf{m}', s} \sum_{\mathbf{n} \neq \mathbf{n}', s'} T(\mathbf{m} - \mathbf{m}') T(\mathbf{n} - \mathbf{n}') \times \quad (102)$$

$$c_{\mathbf{m}s}^\dagger c_{\mathbf{m}'s} c_{\mathbf{n}s'}^\dagger c_{\mathbf{n}'s'} \int_0^\infty dt e^{-i\Delta t} \Phi_{\mathbf{m}\mathbf{m}'}^{\mathbf{n}\mathbf{n}'}(t).$$

Here $\Phi_{\mathbf{m}\mathbf{m}'}^{\mathbf{n}\mathbf{n}'}(t)$ is a multiphonon correlator,

$$\Phi_{\mathbf{m}\mathbf{m}'}^{\mathbf{n}\mathbf{n}'}(t) \equiv \left\langle \left\langle \hat{X}_i^\dagger(t) \hat{X}_{i'}(t) \hat{X}_j^\dagger \hat{X}_{j'} \right\rangle \right\rangle. \quad (103)$$

$\hat{X}_i^\dagger(t)$ and $\hat{X}_{i'}(t)$ commute for any $\gamma(\mathbf{q}, \nu) = \gamma(-\mathbf{q}, \nu)$. \hat{X}_j^\dagger and $\hat{X}_{j'}$ commute as well, so that we can write

$$\hat{X}_i^\dagger(t) \hat{X}_{i'}(t) = \prod_{\mathbf{q}} e^{[u_{i'}(\mathbf{q}, t) - u_i(\mathbf{q}, t)] d_{\mathbf{q}} - H.c.}, \quad (104)$$

$$\hat{X}_j^\dagger \hat{X}_{j'} = \prod_{\mathbf{q}} e^{[u_{j'}(\mathbf{q}) - u_j(\mathbf{q})] d_{\mathbf{q}} - H.c.}, \quad (105)$$

where the phonon branch index ν is dropped for transparency. Applying twice the identity Eq.(52) yields

$$\hat{X}_i^\dagger(t)\hat{X}_{i'}(t)\hat{X}_j^\dagger\hat{X}_{j'} = \prod_{\mathbf{q}} e^{\beta^* d_{\mathbf{q}}^\dagger} e^{-\beta d_{\mathbf{q}}} e^{-|\beta|^2/2} \times \quad (106)$$

$$e^{[u_{i'}(\mathbf{q},t)-u_i(\mathbf{q},t)][u_{j'}^*(\mathbf{q})-u_j^*(\mathbf{q})]/2-H.c.},$$

where

$$\beta = u_i(\mathbf{q},t) - u_{i'}(\mathbf{q},t) + u_j(\mathbf{q}) - u_{j'}(\mathbf{q}).$$

Finally using the average Eq.(54) we find

$$\Phi_{\mathbf{m}\mathbf{m}'}^{\mathbf{n}\mathbf{n}'}(t) = e^{-g^2(\mathbf{m}-\mathbf{m}')} e^{-g^2(\mathbf{n}-\mathbf{n}')} \times \quad (107)$$

$$\exp \left\{ \frac{1}{2N} \sum_{\mathbf{q},\nu} |\gamma(\mathbf{q},\nu)|^2 F_{\mathbf{q}}(\mathbf{m}, \mathbf{m}', \mathbf{n}, \mathbf{n}') \frac{\cosh [\omega_{\mathbf{q}\nu} (\frac{1}{2T} - it)]}{\sinh [\frac{\omega_{\mathbf{q}\nu}}{2T}]} \right\},$$

where

$$F_{\mathbf{q}}(\mathbf{m}, \mathbf{m}', \mathbf{n}, \mathbf{n}') = \cos[\mathbf{q} \cdot (\mathbf{n}' - \mathbf{m})] + \cos[\mathbf{q} \cdot (\mathbf{n} - \mathbf{m}')] - \quad (108)$$

$$\cos[\mathbf{q} \cdot (\mathbf{n}' - \mathbf{m}')] - \cos[\mathbf{q} \cdot (\mathbf{n} - \mathbf{m})].$$

Taking into account that there are only bipolarons in the subspace, where H_b operates, we finally rewrite the Hamiltonian in terms of the creation $b_{\mathbf{m}}^\dagger = c_{\mathbf{m}\uparrow}^\dagger c_{\mathbf{m}\downarrow}^\dagger$ and annihilation $b_{\mathbf{m}} = c_{\mathbf{m}\downarrow} c_{\mathbf{m}\uparrow}$ operators of singlet pairs as

$$H_b = - \sum_{\mathbf{m}} \left[\Delta + \frac{1}{2} \sum_{\mathbf{m}'} v^{(2)}(\mathbf{m} - \mathbf{m}') \right] n_{\mathbf{m}} + \quad (109)$$

$$\sum_{\mathbf{m} \neq \mathbf{m}'} \left[t(\mathbf{m} - \mathbf{m}') b_{\mathbf{m}}^\dagger b_{\mathbf{m}'} + \frac{1}{2} \bar{v}(\mathbf{m} - \mathbf{m}') n_{\mathbf{m}} n_{\mathbf{m}'} \right].$$

There are no triplet pairs in the Holstein model, because the Pauli exclusion principle does not allow two electrons with the same spin to occupy the same site. Here $n_{\mathbf{m}} = b_{\mathbf{m}}^\dagger b_{\mathbf{m}}$ is the bipolaron site-occupation operator,

$$\bar{v}(\mathbf{m} - \mathbf{m}') = 4v(\mathbf{m} - \mathbf{m}') + v^{(2)}(\mathbf{m} - \mathbf{m}'), \quad (110)$$

is the bipolaron-bipolaron interaction including the direct polaron-polaron interaction $v(\mathbf{m} - \mathbf{m}')$ and a second order in $T(\mathbf{m})$ repulsive correlation

$$v^{(2)}(\mathbf{m} - \mathbf{m}') = 2i \int_0^\infty dt e^{-i\Delta t} \Phi_{\mathbf{m}\mathbf{m}'}^{\mathbf{m}'\mathbf{m}}(t). \quad (111)$$

This additional repulsion appears because a virtual hop of one of two polarons of the pair is forbidden, if the neighbouring site is occupied by another pair. The bipolaron transfer integral is of the second order in $T(\mathbf{m})$

$$t(\mathbf{m} - \mathbf{m}') = -2iT^2(\mathbf{m} - \mathbf{m}') \int_0^\infty dt e^{-i\Delta t} \Phi_{\mathbf{m}\mathbf{m}'}^{\mathbf{m}\mathbf{m}'}(t). \quad (112)$$

The *bipolaronic* Hamiltonian, Eq.(109) describes the low-energy physics of strongly coupled electrons and phonons. Using the explicit form of the multi-phonon correlator, Eq.(107), we obtain for dispersionless phonons at $T \ll \omega_0$,

$$\begin{aligned}\Phi_{\mathbf{m}\mathbf{m}'}^{\mathbf{m}\mathbf{m}'}(t) &= e^{-2g^2(\mathbf{m}-\mathbf{m}')} \exp[-2g^2(\mathbf{m}-\mathbf{m}')e^{-i\omega_0 t}], \\ \Phi_{\mathbf{m}\mathbf{m}'}^{\mathbf{m}'\mathbf{m}}(t) &= e^{-2g^2(\mathbf{m}-\mathbf{m}')} \exp[2g^2(\mathbf{m}-\mathbf{m}')e^{-i\omega_0 t}].\end{aligned}$$

Expanding the time-dependent exponents in the Fourier series and calculating the integrals in Eqs.(112) and (111) yield [78]

$$t(\mathbf{m}) = -\frac{2T^2(\mathbf{m})}{\Delta} e^{-2g^2(\mathbf{m})} \sum_{l=0}^{\infty} \frac{[-2g^2(\mathbf{m})]^l}{l!(1+l\omega_0/\Delta)} \quad (113)$$

and

$$v^{(2)}(\mathbf{m}) = \frac{2T^2(\mathbf{m})}{\Delta} e^{-2g^2(\mathbf{m})} \sum_{l=0}^{\infty} \frac{[2g^2(\mathbf{m})]^l}{l!(1+l\omega_0/\Delta)}. \quad (114)$$

When $\Delta \ll \omega_0$, we can keep the first term only with $l = 0$ in the bipolaron hopping integral, Eq.(113). In this case the bipolaron half-bandwidth $zt(\mathbf{a})$ is of the order of $2w^2/(z\Delta)$. However, if the bipolaron binding energy is large, $\Delta \gg \omega_0$, the bipolaron bandwidth dramatically decreases proportionally to e^{-4g^2} in the limit $\Delta \rightarrow \infty$. However, this limit is not realistic because $\Delta = 2E_p - V_c < 2g^2\omega_0$. In a more realistic regime, $\omega_0 < \Delta < 2g^2\omega_0$, Eq.(113) yields

$$t(\mathbf{m}) \approx \frac{2\sqrt{2\pi}T^2(\mathbf{m})}{\sqrt{\omega_0\Delta}} \exp\left[-2g^2 - \frac{\Delta}{\omega_0} \left(1 + \ln \frac{2g^2(\mathbf{m})\omega_0}{\Delta}\right)\right]. \quad (115)$$

On the contrary, the bipolaron-bipolaron repulsion, Eq.(114) has no small exponent in the limit $\Delta \rightarrow \infty$, $v^{(2)} \propto D^2/\Delta$. Together with the direct Coulomb repulsion the second order $v^{(2)}$ ensures stability of the bipolaronic liquid against clustering.

The high temperature behavior of the bipolaron bandwidth is just the opposite to that of the small polaron bandwidth. While the polaron band collapses with increasing temperature [9], the bipolaron band becomes wider [79],

$$t(\mathbf{m}) \propto \frac{1}{\sqrt{T}} \exp\left[-\frac{E_p + \Delta}{2T}\right] \quad (116)$$

for $T > \omega_0$.

7.2 Superlight intersite bipolarons in the Fröhlich-Coulomb model (FCM)

Any realistic theory of doped ionic insulators must include both the long-range Coulomb repulsion between carriers and the strong long-range electron-phonon interaction. From a theoretical standpoint, the inclusion of the long-range Coulomb repulsion is critical in ensuring that the carriers would not

form clusters. Indeed, in order to form stable bipolarons, the e-ph interaction has to be strong enough to overcome the Coulomb repulsion at short distances. Since the realistic e-ph interaction is long-ranged, there is a potential possibility for clustering. The inclusion of the Coulomb repulsion V_c makes the clusters unstable. More precisely, there is a certain window of V_c/E_p inside which the clusters are unstable but mobile bipolarons form nonetheless. In this parameter window bipolarons repel each other and propagate in a narrow band.

Let us consider a generic "Fröhlich-Coulomb" Hamiltonian, which explicitly includes the infinite-range Coulomb and electron-phonon interactions, in a particular lattice structure [80]. The implicitly present infinite Hubbard U prohibits double occupancy and removes the need to distinguish the fermionic spin, as soon as we are interested in the charge excitations alone. Introducing spinless fermion operators $c_{\mathbf{n}}$ and phonon operators $d_{\mathbf{m}\nu}$, the Hamiltonian is written as

$$\begin{aligned} H = & \sum_{\mathbf{n} \neq \mathbf{n}'} T(\mathbf{n} - \mathbf{n}') c_{\mathbf{n}}^\dagger c_{\mathbf{n}'} + \frac{1}{2} \sum_{\mathbf{n} \neq \mathbf{n}'} V_c(\mathbf{n} - \mathbf{n}') c_{\mathbf{n}}^\dagger c_{\mathbf{n}} c_{\mathbf{n}'}^\dagger c_{\mathbf{n}'} + \quad (117) \\ & \omega_0 \sum_{\mathbf{n} \neq \mathbf{m}, \nu} g_\nu(\mathbf{m} - \mathbf{n})(\mathbf{e}_\nu \cdot \mathbf{e}_{\mathbf{m}-\mathbf{n}}) c_{\mathbf{n}}^\dagger c_{\mathbf{n}} (d_{\mathbf{m}\nu}^\dagger + d_{\mathbf{m}\nu}) + \\ & \omega_0 \sum_{\mathbf{m}, \nu} \left(d_{\mathbf{m}\nu}^\dagger d_{\mathbf{m}\nu} + \frac{1}{2} \right). \end{aligned}$$

The e-ph term is written in the real space representation (section 2), which is more convenient in working with complex lattices.

In general, the many-body model Eq.(117) is of considerable complexity. However, we are interested in the non/near adiabatic limit of the strong e-ph interaction. In this case, the kinetic energy is a perturbation and the model can be grossly simplified using the Lang-Firsov canonical transformation in the Wannier representation for electrons and phonons,

$$S = \sum_{\mathbf{m} \neq \mathbf{n}, \nu} g_\nu(\mathbf{m} - \mathbf{n})(\mathbf{e}_\nu \cdot \mathbf{e}_{\mathbf{m}-\mathbf{n}}) c_{\mathbf{n}}^\dagger c_{\mathbf{n}} (d_{\mathbf{m}\nu}^\dagger - d_{\mathbf{m}\nu}).$$

The transformed Hamiltonian is

$$\begin{aligned} \tilde{H} = e^{-S} H e^S = & \sum_{\mathbf{n} \neq \mathbf{n}'} \hat{\sigma}_{\mathbf{n}\mathbf{n}'} c_{\mathbf{n}}^\dagger c_{\mathbf{n}'} + \omega_0 \sum_{\mathbf{m}\alpha} \left(d_{\mathbf{m}\alpha}^\dagger d_{\mathbf{m}\alpha} + \frac{1}{2} \right) + \quad (118) \\ & \sum_{\mathbf{n} \neq \mathbf{n}'} v(\mathbf{n} - \mathbf{n}') c_{\mathbf{n}}^\dagger c_{\mathbf{n}} c_{\mathbf{n}'}^\dagger c_{\mathbf{n}'} - E_p \sum_{\mathbf{n}} c_{\mathbf{n}}^\dagger c_{\mathbf{n}}. \end{aligned}$$

The last term describes the energy gained by polarons due to e-ph interaction. E_p is the familiar polaron level shift,

$$E_p = \omega \sum_{\mathbf{m}\nu} g_\nu^2(\mathbf{m} - \mathbf{n})(\mathbf{e}_\nu \cdot \mathbf{e}_{\mathbf{m}-\mathbf{n}})^2, \quad (119)$$

which is independent of \mathbf{n} . The third term on the right-hand side in Eq.(130) is the polaron-polaron interaction:

$$v(\mathbf{n} - \mathbf{n}') = V_c(\mathbf{n} - \mathbf{n}') - V_{ph}(\mathbf{n} - \mathbf{n}'), \quad (120)$$

where

$$V_{ph}(\mathbf{n} - \mathbf{n}') = 2\omega_0 \sum_{\mathbf{m}, \nu} g_\nu(\mathbf{m} - \mathbf{n}) g_\nu(\mathbf{m} - \mathbf{n}') \times (\mathbf{e}_\nu \cdot \mathbf{e}_{\mathbf{m}-\mathbf{n}})(\mathbf{e}_\nu \cdot \mathbf{e}_{\mathbf{m}-\mathbf{n}'}).$$

The phonon-induced interaction V_{ph} is due to displacements of common ions by two electrons. The transformed hopping operator $\hat{\sigma}_{\mathbf{n}\mathbf{n}'}$ in the first term in Eq.(118) is given by

$$\hat{\sigma}_{\mathbf{n}\mathbf{n}'} = T(\mathbf{n} - \mathbf{n}') \exp \left[\sum_{\mathbf{m}, \nu} [g_\nu(\mathbf{m} - \mathbf{n})(\mathbf{e}_\nu \cdot \mathbf{e}_{\mathbf{m}-\mathbf{n}}) - g_\nu(\mathbf{m} - \mathbf{n}')(\mathbf{e}_\nu \cdot \mathbf{e}_{\mathbf{m}-\mathbf{n}'})] (d_{\mathbf{m}\alpha}^\dagger - d_{\mathbf{m}\alpha}) \right]. \quad (121)$$

This term perturbation at large λ . Here we consider a particular lattice structure (ladder), where bipolarons tunnel already in the first order in $T(\mathbf{n})$, so that $\hat{\sigma}_{\mathbf{n}\mathbf{n}'}$ can be averaged over phonons. When $T \ll \omega_0$ the result is

$$t(\mathbf{n} - \mathbf{n}') \equiv \langle \langle \hat{\sigma}_{\mathbf{n}\mathbf{n}'} \rangle \rangle_{ph} = T(\mathbf{n} - \mathbf{n}') \exp[-g^2(\mathbf{n} - \mathbf{n}')], \quad (122)$$

$$g^2(\mathbf{n} - \mathbf{n}') = \sum_{\mathbf{m}, \nu} g_\nu(\mathbf{m} - \mathbf{n})(\mathbf{e}_\nu \cdot \mathbf{e}_{\mathbf{m}-\mathbf{n}}) \times [g_\nu(\mathbf{m} - \mathbf{n})(\mathbf{e}_\nu \cdot \mathbf{e}_{\mathbf{m}-\mathbf{n}}) - g_\nu(\mathbf{m} - \mathbf{n}')(\mathbf{e}_\nu \cdot \mathbf{e}_{\mathbf{m}-\mathbf{n}'})].$$

The mass renormalization exponent can be expressed via E_p and V_{ph} as

$$g^2(\mathbf{n} - \mathbf{n}') = \frac{1}{\omega_0} \left[E_p - \frac{1}{2} V_{ph}(\mathbf{n} - \mathbf{n}') \right]. \quad (123)$$

Now phonons are "integrated out" and the polaronic Hamiltonian is given by

$$H_p = H_0 + H_{pert}, \quad (124)$$

$$H_0 = -E_p \sum_{\mathbf{n}} c_{\mathbf{n}}^\dagger c_{\mathbf{n}} + \frac{1}{2} \sum_{\mathbf{n} \neq \mathbf{n}'} v(\mathbf{n} - \mathbf{n}') c_{\mathbf{n}}^\dagger c_{\mathbf{n}} c_{\mathbf{n}'}^\dagger c_{\mathbf{n}'},$$

$$H_{pert} = \sum_{\mathbf{n} \neq \mathbf{n}'} t(\mathbf{n} - \mathbf{n}') c_{\mathbf{n}}^\dagger c_{\mathbf{n}'},$$

When V_{ph} exceeds V_c the full interaction becomes negative and polarons form pairs. The real space representation allows us to elaborate more physics behind

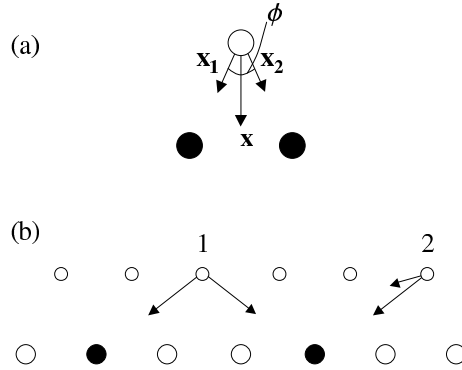


Fig. 4. Mechanism of the polaron-polaron interaction. (a) Together, two polarons (solid circles) deform the lattice more effectively than separately. An effective attraction occurs when the angle ϕ between \mathbf{x}_1 and \mathbf{x}_2 is less than $\pi/2$. (b) A mixed situation: ion 1 results in repulsion between two polarons while ion 2 results in attraction.

the lattice sums in Eq.(119) and Eq.(120) [80]. When a carrier (electron or hole) acts on an ion with a force \mathbf{f} , it displaces the ion by some vector $\mathbf{x} = \mathbf{f}/k$. Here k is the ion's force constant. The total energy of the carrier-ion pair is $-\mathbf{f}^2/(2k)$. This is precisely the summand in Eq.(119) expressed via dimensionless coupling constants. Now consider two carriers interacting with the *same* ion, Fig.4a. The ion displacement is $\mathbf{x} = (\mathbf{f}_1 + \mathbf{f}_2)/k$ and the energy is $-\mathbf{f}_1^2/(2k) - \mathbf{f}_2^2/(2k) - (\mathbf{f}_1 \cdot \mathbf{f}_2)/k$. Here the last term should be interpreted as an ion-mediated interaction between the two carriers. It depends on the scalar product of \mathbf{f}_1 and \mathbf{f}_2 and consequently on the relative positions of the carriers with respect to the ion. If the ion is an isotropic harmonic oscillator, as we assume here, then the following simple rule applies. If the angle ϕ between \mathbf{f}_1 and \mathbf{f}_2 is less than $\pi/2$ the polaron-polaron interaction will be attractive, if otherwise it will be repulsive. In general, some ions will generate attraction, and some repulsion between polarons, Fig. 4b.

The overall sign and magnitude of the interaction is given by the lattice sum in Eq.(120), the evaluation of which is elementary. One should also note that according to Eq.(123) an attractive e-ph interaction reduces the polaron mass (and consequently the bipolaron mass), while repulsive e-ph interaction enhances the mass. Thus, the long-range nature of the e-ph interaction serves a double purpose. Firstly, it generates an additional inter-polaron attraction because the distant ions have small angle ϕ . This additional attraction helps to overcome the direct Coulomb repulsion between polarons. And secondly, the Fröhlich interaction makes the bipolarons lighter.

The many-particle ground state of H_0 depends on the sign of the polaron-polaron interaction, the carrier density, and the lattice geometry. Here we consider the zig-zag ladder, Fig.5a, assuming that all sites are isotropic two-dimensional harmonic oscillators. For simplicity, we also adopt the nearest-neighbour approximation for both interactions, $g_\nu(\mathbf{l}) \equiv g$, $V_c(\mathbf{n}) \equiv V_c$, and for the hopping integrals, $T(\mathbf{m}) = T_{NN}$ for $l = n = m = a$, and zero otherwise. Hereafter we set the lattice period $a = 1$. There are four nearest neighbours in the ladder, $z = 4$. Then the *one-particle* polaronic Hamiltonian takes the form

$$H_p = -E_p \sum_n (c_n^\dagger c_n + p_n^\dagger p_n) + \sum_n [t'(c_{n+1}^\dagger c_n + p_{n+1}^\dagger p_n) + t(p_n^\dagger c_n + p_{n-1}^\dagger c_n) + H.c.], \quad (125)$$

where c_n and p_n are polaron annihilation operators on the lower and upper legs of the ladder, respectively, Fig.5b. Using Eqs.(119), (120) and (123) we find

$$\begin{aligned} E_p &= 4g^2\omega_0, \\ t' &= T_{NN} \exp\left(-\frac{7E_p}{8\omega_0}\right), \\ t &= T_{NN} \exp\left(-\frac{3E_p}{4\omega_0}\right). \end{aligned} \quad (126)$$

The Fourier transform of Eq.(125) into momentum space yields

$$H_p = \sum_k (2t' \cos k - E_p)(c_k^\dagger c_k + p_k^\dagger p_k) + t \sum_k [(1 + e^{ik})p_k^\dagger c_k + H.c.]. \quad (127)$$

A linear transformation of c_k and p_k diagonalises the Hamiltonian. There are two overlapping polaronic bands,

$$E_1(k) = -E_p + 2t' \cos(k) \pm 2t \cos(k/2) \quad (128)$$

with the effective mass $m^* = 2/|4t' \pm t|$ near their edges.

Let us now place two polarons on the ladder. The nearest neighbour interaction is $v = V_c - E_p/2$, if two polarons are on different legs of the ladder, and $v = V_c - E_p/4$, if both polarons are on the same leg. The attractive interaction is provided via the displacement of the lattice sites, which are the common nearest neighbours to both polarons. There are two such nearest neighbours for the intersite bipolaron of type *A* or *B*, Fig.5c, but there is only one common nearest neighbour for bipolaron *C*, Fig.5d. When $V_c > E_p/2$, there are no bound states and the multi-polaron system is a one-dimensional Luttinger

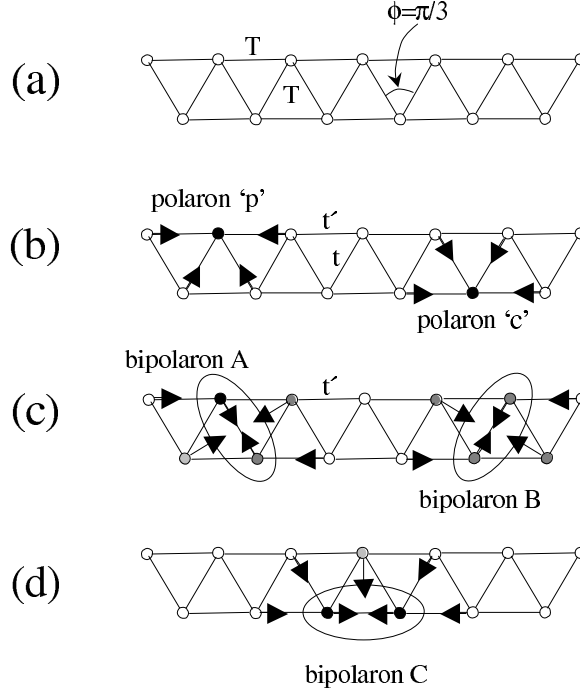


Fig. 5. One-dimensional zig-zag ladder. (a) Initial ladder with the bare hopping amplitude $T(a)$. (b) Two types of polarons with their respective deformations. (c) Two degenerate bipolaron configurations A and B. (d) A different bipolaron configuration, C, whose energy is higher than that of A and B.

liquid. However, when $V_c < E_p/2$ and consequently $v < 0$, the two polarons are bound into an inter-site bipolaron of types *A* or *B*.

It is quite remarkable that the bipolaron tunnelling in the ladder already appears in the first order with respect to a single-electron tunnelling. This case is different from both onsite bipolarons discussed above, and from intersite chain bipolarons of Ref. [81], where the bipolaron tunnelling was of the second order in $T(a)$. Indeed, the lowest energy degenerate configurations *A* and *B* are degenerate. They are coupled by H_{pert} . Neglecting all higher-energy configurations, we can project the Hamiltonian onto the subspace containing *A*, *B*, and empty sites.

The result of such a projection is the bipolaronic Hamiltonian

$$H_b = \left(V_c - \frac{5}{2} E_p \right) \sum_n [A_n^\dagger A_n + B_n^\dagger B_n] - t' \sum_n [B_n^\dagger A_n + B_{n-1}^\dagger A_n + H.c.], \quad (129)$$

where $A_n = c_n p_n$ and $B_n = p_n c_{n+1}$ are intersite bipolaron annihilation operators, and the bipolaron-bipolaron interaction is dropped (see below). The

Fourier transform of Eq.(129) yields two *bipolaron* bands,

$$E_2(k) = V_c - \frac{5}{2}E_p \pm 2t' \cos(k/2). \quad (130)$$

with a combined width $4|t'|$. The bipolaron binding energy in zero order with respect to t, t' is

$$\Delta \equiv 2E_1(0) - E_2(0) = \frac{E_p}{2} - V_c. \quad (131)$$

The bipolaron mass near the bottom of the lowest band, $m^{**} = 2/t'$, is

$$m^{**} = 4m^* \left[1 + 0.25 \exp\left(\frac{E_p}{8\omega_0}\right) \right]. \quad (132)$$

The numerical coefficient $1/8$ in the exponent ensures that m^{**} remains of the order of m^* even at large E_p . This fact combines with a weaker renormalization of m^* providing a *superlight* bipolaron.

In models with strong intersite attraction there is a possibility of clusterisation. Similar to the two-particle case above, the lowest energy of n polarons placed on the nearest neighbours of the ladder is found as

$$E_n = (2n - 3)V_c - \frac{6n - 1}{4}E_p \quad (133)$$

for any $n \geq 3$. There are *no* resonating states for a n -polaron configuration if $n \geq 3$. Therefore there is no first-order kinetic energy contribution to their energy. E_n should be compared with the energy $E_1 + (n - 1)E_2/2$ of far separated $(n - 1)/2$ bipolarons and a single polaron for odd $n \geq 3$, or with the energy of far separated n bipolarons for even $n \geq 4$. ‘‘Odd’’ clusters are stable if

$$V_c < \frac{n}{6n - 10}E_p, \quad (134)$$

and ‘‘even’’ clusters are stable if

$$V_c < \frac{n - 1}{6n - 12}E_p. \quad (135)$$

As a result we find that bipolarons repel each other and single polarons at $V_c > 3E_p/8$. If V_c is less than $3E_p/8$ then immobile bound clusters of three and more polarons could form. One should notice that at distances much larger than the lattice constant the polaron-polaron interaction is always repulsive, and the formation of infinite clusters, stripes or strings is impossible (see also [47]). Combining the condition of bipolaron formation and that of the instability of larger clusters we obtain a window of parameters

$$\frac{3}{8}E_p < V_c < \frac{1}{2}E_p, \quad (136)$$

where the ladder is a bipolaronic conductor. Outside the window the ladder is either charge-segregated into finite-size clusters (small V_c), or it is a liquid of repulsive polarons (large V_c).

There is strong experimental evidence for superlight intersite bipolarons in cuprate superconductors (see below), where they form in-plane oxygen - apex oxygen pairs (so called apex bipolarons) and/or in-plane oxygen-oxygen pairs [40, 82, 80]. While the long-range Fröhlich interaction combined with Coulomb repulsion might cause clustering of polarons into finite-size quasi-metallic mesoscopic textures, the analytical [83] and QMC [84] studies of mesoscopic textures with lattice deformations and Coulomb repulsion show that pairs dominate over phase separation since bipolarons effectively repel each other (see also [47]).

8 Bipolaronic superconductivity

In the subspace with no single polarons, the Hamiltonian of electrons strongly-coupled with phonons is reduced to the bipolaronic Hamiltonian written in terms of creation, $b_{\mathbf{m}}^\dagger = c_{\mathbf{m}\uparrow}^\dagger c_{\mathbf{m}\downarrow}^\dagger$ and annihilation, $b_{\mathbf{m}}$, bipolaron operators as

$$H_b = \sum_{\mathbf{m} \neq \mathbf{m}'} \left[t(\mathbf{m} - \mathbf{m}') b_{\mathbf{m}}^\dagger b_{\mathbf{m}'} + \frac{1}{2} \bar{v}(\mathbf{m} - \mathbf{m}') n_{\mathbf{m}} n_{\mathbf{m}'} \right], \quad (137)$$

where $\bar{v}(\mathbf{m} - \mathbf{m}')$ is the bipolaron-bipolaron interaction, $n_{\mathbf{m}} = b_{\mathbf{m}}^\dagger b_{\mathbf{m}}$, and the position of the middle of the bipolaron band is taken as zero. There are additional spin quantum numbers $S = 0, 1$; $S_z = 0, \pm 1$, which should be added to the definition of $b_{\mathbf{m}}$ in the case of intersite bipolarons, which tunnel via the one-particle hopping. This "crab-like" tunnelling, Fig.5, results in a bipolaron bandwidth of the same order as the polaron one. Keeping this in mind we can apply H_b , Eq.(137) to both on-site and/or inter-site bipolarons, and even to more extended non-overlapping pairs, implying that the site index \mathbf{m} is the position of the centre of mass of a pair.

Bipolarons are not perfect bosons. In the subspace of pairs and empty sites their operators commute as

$$b_{\mathbf{m}} b_{\mathbf{m}}^\dagger + b_{\mathbf{m}}^\dagger b_{\mathbf{m}} = 1, \quad (138)$$

$$b_{\mathbf{m}} b_{\mathbf{m}'}^\dagger - b_{\mathbf{m}'}^\dagger b_{\mathbf{m}} = 0 \quad (139)$$

for $\mathbf{m} \neq \mathbf{m}'$. This makes useful the pseudospin analogy [41],

$$b_{\mathbf{m}}^\dagger = S_{\mathbf{m}}^x - i S_{\mathbf{m}}^y \quad (140)$$

and

$$b_{\mathbf{m}}^\dagger b_{\mathbf{m}} = \frac{1}{2} - S_{\mathbf{m}}^z \quad (141)$$

with the pseudospin 1/2 operators $S^{x,y,z} = \frac{1}{2} \tau_{1,2,3}$. $S_{\mathbf{m}}^z = 1/2$ corresponds to an empty site \mathbf{m} and $S_{\mathbf{m}}^z = -1/2$ to a site occupied by the bipolaron. Spin operators preserve the bosonic nature of bipolarons, when they are on

different sites, and their fermionic internal structure. Replacing bipolarons by spin operators we transform the bipolaronic Hamiltonian into the anisotropic Heisenberg Hamiltonian,

$$H_b = \sum_{\mathbf{m} \neq \mathbf{m}'} \left[\frac{1}{2} \bar{v}_{\mathbf{m}\mathbf{m}'} S_{\mathbf{m}}^z S_{\mathbf{m}'}^z + t_{\mathbf{m}\mathbf{m}'} (S_{\mathbf{m}}^x S_{\mathbf{m}'}^x + S_{\mathbf{m}}^y S_{\mathbf{m}'}^y) \right]. \quad (142)$$

This Hamiltonian has been investigated in detail as a relevant form for magnetism and also for quantum solids like a lattice model of ${}^4\text{He}$. However, while in those cases the magnetic field is an independent thermodynamic variable, in our case the total ‘‘magnetization’’ is fixed,

$$\frac{1}{N} \sum_{\mathbf{m}} \langle \langle S_{\mathbf{m}}^z \rangle \rangle = \frac{1}{2} - n_b, \quad (143)$$

if the bipolaron density n_b is conserved. Spin 1/2 Heisenberg Hamiltonian, Eq.(142) cannot be solved analytically. Complicated commutation rules for bipolaron operators make the problem hard, but not in the limit of low atomic density of bipolarons, $n_b \ll 1$ (for a complete phase diagram of bipolarons on a lattice see Refs. [41, 85]). In this limit we can reduce the problem to a charged Bose gas on a lattice [86]. Let us transform the bipolaronic Hamiltonian to a representation containing only the Bose operators $a_{\mathbf{m}}$ and $a_{\mathbf{m}}^\dagger$ defined as

$$b_{\mathbf{m}} = \sum_{k=0}^{\infty} \beta_k (a_{\mathbf{m}}^\dagger)^k a_{\mathbf{m}}^{k+1}, \quad (144)$$

$$b_{\mathbf{m}}^\dagger = \sum_{k=0}^{\infty} \beta_k (a_{\mathbf{m}}^\dagger)^{k+1} a_{\mathbf{m}}^k, \quad (145)$$

where

$$a_{\mathbf{m}} a_{\mathbf{m}'}^\dagger - a_{\mathbf{m}'}^\dagger a_{\mathbf{m}} = \delta_{\mathbf{m}, \mathbf{m}'}. \quad (146)$$

The first few coefficients β_k are found by substituting Eqs.(144) and (145) into Eqs.(138) and (139),

$$\beta_0 = 1, \beta_1 = -1, \beta_2 = \frac{1}{2} + \frac{\sqrt{3}}{6}. \quad (147)$$

We also introduce bipolaron and boson Ψ -operators as

$$\Phi(\mathbf{r}) = \frac{1}{\sqrt{N}} \sum_{\mathbf{m}} \delta(\mathbf{r} - \mathbf{m}) b_{\mathbf{m}}, \quad (148)$$

$$\Psi(\mathbf{r}) = \frac{1}{\sqrt{N}} \sum_{\mathbf{m}} \delta(\mathbf{r} - \mathbf{m}) a_{\mathbf{m}}. \quad (149)$$

The transformation of the field operators takes the form

$$\Phi(\mathbf{r}) = \left[1 - \frac{\Psi^\dagger(\mathbf{r})\Psi(\mathbf{r})}{N} + \frac{(1/2 + \sqrt{3}/6)\Psi^\dagger(\mathbf{r})\Psi^\dagger(\mathbf{r})\Psi(\mathbf{r})\Psi(\mathbf{r})}{N^2} + \dots \right] \Psi(\mathbf{r}). \quad (150)$$

Then we write the bipolaronic Hamiltonian as

$$H_b = \int d\mathbf{r} \int d\mathbf{r}' \Psi^\dagger(\mathbf{r}) t(\mathbf{r} - \mathbf{r}') \Psi(\mathbf{r}') + H_d + H_h + H^{(3)}, \quad (151)$$

where

$$H_d = \frac{1}{2} \int d\mathbf{r} \int d\mathbf{r}' \bar{v}(\mathbf{r} - \mathbf{r}') \Psi^\dagger(\mathbf{r}) \Psi^\dagger(\mathbf{r}') \Psi(\mathbf{r}') \Psi(\mathbf{r}), \quad (152)$$

is the dynamic part,

$$H_k = \frac{2}{N} \int d\mathbf{r} \int d\mathbf{r}' t(\mathbf{r} - \mathbf{r}') \times \quad (153)$$

$$[\Psi^\dagger(\mathbf{r}) \Psi^\dagger(\mathbf{r}') \Psi(\mathbf{r}') \Psi(\mathbf{r}') + \Psi^\dagger(\mathbf{r}) \Psi^\dagger(\mathbf{r}) \Psi(\mathbf{r}) \Psi(\mathbf{r}')].$$

is the kinematic (hard-core) part due to the "imperfect" commutation rules, and $H^{(3)}$ includes three- and higher-body collisions. Here

$$t(\mathbf{r} - \mathbf{r}') = \sum_{\mathbf{k}} \epsilon_{\mathbf{k}}^{**} e^{i\mathbf{k} \cdot (\mathbf{r} - \mathbf{r}')},$$

$$\bar{v}(\mathbf{r} - \mathbf{r}') = \frac{1}{N} \sum_{\mathbf{k}} \bar{v}_{\mathbf{k}} e^{i\mathbf{k} \cdot (\mathbf{r} - \mathbf{r}')},$$

$\bar{v}_{\mathbf{k}} = \sum_{\mathbf{m} \neq 0} \bar{v}(\mathbf{m}) \exp(i\mathbf{k} \cdot \mathbf{m})$ is the Fourier component of the dynamic interaction and

$$\epsilon_{\mathbf{k}}^{**} = \sum_{\mathbf{m} \neq 0} t(\mathbf{m}) \exp(-i\mathbf{k} \cdot \mathbf{m}) \quad (154)$$

is the bipolaron band dispersion. $H^{(3)}$ contains powers of the field operator higher than four. In the dilute limit, $n_b \ll 1$, only two-particle interactions are essential which include the short-range kinematic and direct density-density repulsions. Because \bar{v} already has the short range part $v^{(2)}$, Eq.(113), the kinematic contribution can be included in the definition of \bar{v} . As a result H_b is reduced to the Hamiltonian of interacting hard-core charged bosons tunnelling in the narrow band.

To describe electrodynamics of bipolarons we introduce the vector potential $\mathbf{A}(\mathbf{r})$ using the so-called Peierls substitution [87],

$$t(\mathbf{m} - \mathbf{m}') \rightarrow t(\mathbf{m} - \mathbf{m}') e^{i2e\mathbf{A}(\mathbf{m}) \cdot (\mathbf{m} - \mathbf{m}')},$$

which is a fair approximation when the magnetic field is weak compared with the atomic field, $eHa^2 \ll 1$. It has the following form,

$$t(\mathbf{r} - \mathbf{r}') \rightarrow t(\mathbf{r}, \mathbf{r}') = \sum_{\mathbf{k}} \epsilon_{\mathbf{k} - 2e\mathbf{A}}^{**} e^{i\mathbf{k} \cdot (\mathbf{r} - \mathbf{r}')} \quad (155)$$

in real space. If the magnetic field is weak, we can expand $\epsilon_{\mathbf{k}}^{**}$ in the vicinity of $\mathbf{k} = 0$ to obtain

$$t(\mathbf{r}, \mathbf{r}') \approx -\frac{[\nabla + 2ie\mathbf{A}(\mathbf{r})]^2}{2m^{**}}\delta(\mathbf{r} - \mathbf{r}'), \quad (156)$$

where

$$\frac{1}{m^{**}} = \left(\frac{d^2 \epsilon_{\mathbf{k}}^{**}}{dk^2} \right)_{k \rightarrow 0} \quad (157)$$

is the inverse bipolaron mass. Here we assume a parabolic dispersion near the bottom of the band, $\epsilon_{\mathbf{k}}^{**} \sim k^2$, so that

$$H_b \approx - \int d\mathbf{r} \Psi^\dagger(\mathbf{r}) \left\{ \frac{[\nabla + 2ie\mathbf{A}(\mathbf{r})]^2}{2m^{**}} + \mu \right\} \Psi(\mathbf{r}) + \quad (158)$$

$$\frac{1}{2} \int d\mathbf{r} d\mathbf{r}' \bar{v}(\mathbf{r} - \mathbf{r}') \Psi^\dagger(\mathbf{r}) \Psi^\dagger(\mathbf{r}') \Psi(\mathbf{r}) \Psi(\mathbf{r}'),$$

where we add the *bipolaron* chemical potential μ . We note that the bipolaron-bipolaron interaction is the Coulomb repulsion, $\bar{v}(\mathbf{r}) \sim 1/(\epsilon_0 r)$ at large distances, and the hard-core repulsion is not important in the dilute limit. The Hamiltonian Eq.(159) describes the charged Bose gas with the effective boson mass m^{**} and charge $2e$, which is a superconductor [88].

9 Bipolaronic superconductivity in cuprates

The fact that Helium-4 and its isotope Helium-3 are well known Bose and Fermi superfluids, respectively, with very different superfluid transition temperatures ($T_c = 2.17K$ in 4He and $T_c = 0.0026K$ in 3He) already kindles the view that high-temperature superconductivity might derive from preformed real-space charged bosons rather than in the BCS state with Cooper pairs, which are correlations in momentum space. The possibility of real-space pairing of carriers in cuprates, as opposed to Cooper pairing, has been the subject of much discussion. Some authors dismissed any real-space pairs even in underdoped cuprates, where a low density of carriers appears to favor individual pairing rather than Cooper pairing. But on the other hand real-space pairing is strongly supported by our strong-coupling extension of the BCS theory since the e-ph interaction is very strong in cuprates. Also on the experimental side a growing number of other independent observations point to the possibility that high- T_c superconductors may not be conventional Bardeen-Cooper-Schrieffer (BCS) superconductors, but rather derive from the Bose-Einstein condensation (BEC) of real-space superlight small bipolarons. There is strong evidence for real-space pairing and the three-dimensional BEC in cuprates from unusual upper critical fields [89] and isotope effects [106] predicted by us and the λ -like electronic specific heat [90], parameter-free fitting of experimental T_c with BEC T_c [91], normal state pseudogaps [92, 93] and anisotropy [94], and

more recently from normal state diamagnetism [95], the Hall-Lorenz numbers [96, 97], the normal state Nernst effect [98, 99], and the giant proximity effect (GPE) [100]. Here I briefly discuss a few of these remarkable observations (for more details see Ref. [23] and Part IV).

9.1 Upper critical field, the Hall-Lorenz number, and isotope effects

Magnetotransport [101] and thermal magnetotransport [102, 96] data strongly support preformed pairs in cuprates. In particular, many high magnetic field studies revealed a non-BCS upward curvature of the upper critical field, $H_{c2}(T)$ and its non-linear temperature dependence in the vicinity of T_c in a number of cuprates as well as in a few other unconventional superconductors, Fig.6. If unconventional superconductors are in the "bosonic" limit of preformed real-space pairs, such unusual critical fields are expected in accordance with the theoretical prediction for the Bose-Einstein condensation of charged bosons in an external magnetic field [89].

Notwithstanding, some "direct" evidence for the existence of a charge $2e$ Bose liquid in the normal state of cuprates is highly desirable. Alexandrov and Mott [103] discussed the thermal conductivity κ ; the contribution from the carriers given by the Wiedemann-Franz ratio depends strongly on the elementary charge as $\sim (e^*)^{-2}$ and should be significantly suppressed in the case of $e^* = 2e$ compared with the Fermi-liquid contribution. As a result, the Lorenz number, $L = (e/k_B)^2 \kappa_e / (T\sigma)$ differs significantly from the Sommerfeld value $L_e = \pi^2/3$ of the standard Fermi-liquid theory, if carriers are double-charged bosons. Here κ_e , σ , and e are the electronic thermal conductivity, the electrical conductivity, and the elementary charge, respectively. Ref. [103] predicted a rather low Lorenz number for bipolarons, $L = 6L_e / (4\pi^2) \approx 0.15L_e$, due to the double charge of carriers, and also due to their nearly classical distribution function above T_c .

The extraction of the electron thermal conductivity has proven difficult since both the electron term, κ_e and the phonon term, κ_{ph} are comparable to each other in the cuprates. A new way to determine the Lorenz number has been realized by Zhang et al. [102], based on the thermal Hall conductivity. The thermal Hall effect allowed for an efficient way to separate the phonon heat current even when it is dominant. As a result, the "Hall" Lorenz number, $L_H = (e/k_B)^2 \kappa_{xy} / (T\sigma_{xy})$, has been directly measured in $YBa_2Cu_3O_{6.95}$ because transverse thermal κ_{xy} and electrical σ_{xy} conductivities involve only the electrons. Remarkably, the measured value of L_H just above T_c is about the same as predicted by the bipolaron model, $L_H \approx 0.15L_e$. The experimental L_H showed a strong temperature dependence, which violates the Wiedemann-Franz law. This experimental observation has been accounted for by taking into account thermally excited polarons and also triplet pairs in the bipolaron model [96], Fig.7.

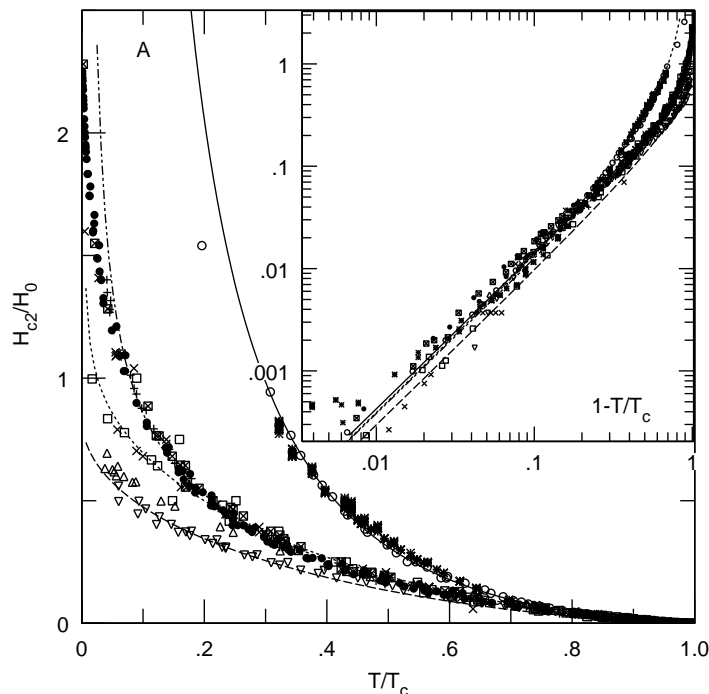


Fig. 6. Resistive upper critical field [101] (determined at 50% of the transition) of cuprates, spin-ladders and organic superconductors scaled according to the Bose-Einstein condensation field of charged bosons [89], $H_{c2}(T) \propto [b(1-t)/t + 1 - t^{1/2}]^{3/2}$ with $t = T/T_c$. The parameter b is proportional to the number of delocalised bosons at zero temperature, b is 1 (solid line), 0.02 (dashed-dotted line), 0.0012 (dotted line), and 0 (dashed line). The inset shows a universal scaling of the same data near T_c on the logarithmic scale. Symbols correspond to $Tl-2201$ (\bullet), $La_{1.85}Sr_{0.15}CuO_4$ (Δ), $Bi-2201$ (\times), $Bi-2212$ ($*$), $YBa_2Cu_3O_{6+x}$ (\circ), $La_{2-x}Ce_xCuO_{4-y}$ (squares), $Sr_2Ca_{12}Cu_{24}O_{41}$ ($+$), and Bechgaard salt organic superconductor (∇).

Another compelling evidence for (bi)polaronic carries in novel superconductors was provided by the discovery of substantial isotope effects on T_c and on the carrier mass [104, 105]. The advances in the fabrication of the isotope substituted samples made it possible to measure a sizable isotope effect, $\alpha = -d \ln T_c / d \ln M$ in many high- T_c oxides. This led to a general conclusion that phonons are relevant for high T_c . Moreover the isotope effect in cuprates was found to be quite different from the BCS prediction, $\alpha = 0.5$ (or less). Several compounds showed $\alpha > 0.5$, and sometimes negative values of α were observed.

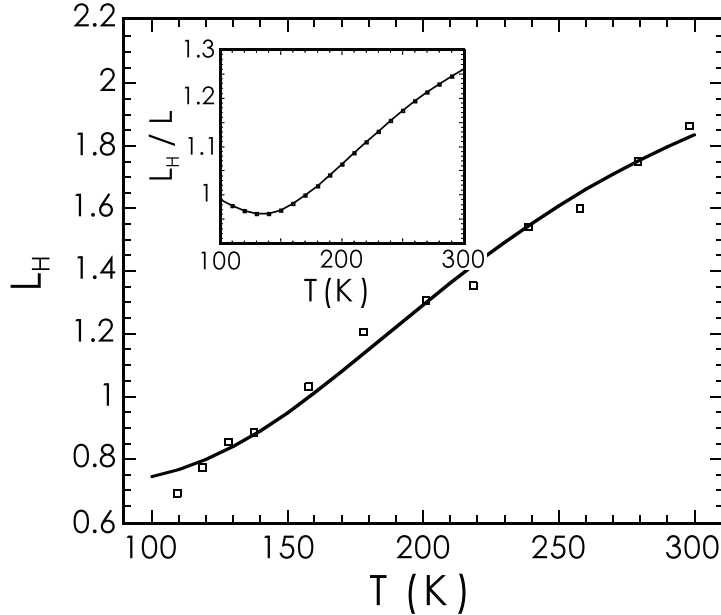


Fig. 7. The Hall Lorenz number L_H [96] of charged bosons fits the experiment in $\text{YBa}_2\text{Cu}_3\text{O}_{6.95}$ [102]. The pseudogap is taken as 675 K. The inset gives the ratio of the Hall Lorenz number to the Lorenz number in the model.

Essential features of the isotope effect, in particular large values in low T_c cuprates, an overall trend to lower value as T_c increases, and a small or even negative α in some high T_c cuprates can be understood in the framework of the bipolaron theory [106]. With increasing ion mass the bipolaron mass increases and the Bose-Einstein condensation temperature $T_c \propto 1/m^{**}$ decreases in the bipolaronic superconductor (section 8). On the contrary in polaronic superconductors (section 6) an increase of the ion mass leads to a band narrowing enhancing the polaron density of states and increasing T_c . Hence the isotope exponent of T_c can distinguish the BCS like polaronic superconductivity with $\alpha < 0$, and the Bose-Einstein condensation of small bipolarons with $\alpha > 0$. Moreover, underdoped cuprates, which are certainly in the BEC regime, could have $\alpha > 0.5$, as observed.

The isotope effect on T_c is linked with the isotope effect on the carrier mass, α_{m^*} , as [106]

$$\alpha = -d \ln T_c / d \ln M = \alpha_{m^*} [1 - Z / (\lambda - \mu_c)], \quad (159)$$

where $\alpha_{m^*} = d \ln m^* / d \ln M$ and $Z = m / m^* \ll 1$. In ordinary metals, where the Migdal approximation is believed to be valid, the renormalized effective mass of electrons is independent of the ion mass M because the electron-phonon interaction constant λ does not depend on M . However, when the

e-ph interaction is sufficiently strong, the electrons form polarons dressed by lattice distortions, with an effective mass $m^* = m \exp(\gamma E_p/\omega)$. While E_p in the above expression does not depend on the ion mass, the phonon frequency does. As a result, there is a large isotope effect on the carrier mass in polaronic conductors, $\alpha_{m^*} = (1/2) \ln(m^*/m)$ [106], in contrast to the zero isotope effect in ordinary metals. Such an effect was observed in cuprates in the London penetration depth λ_H of isotope-substituted samples [104]. The carrier density is unchanged with the isotope substitution of O^{16} by O^{18} , so that the isotope effect on λ_H measures directly the isotope effect on the carrier mass. In particular, the carrier mass isotope exponent α_{m^*} was found as large as $\alpha_{m^*} = 0.8$ in $La_{1.895}Sr_{0.105}CuO_4$.

More recent high resolution angle resolved photoemission spectroscopy [107] provided another compelling evidence for a strong e-ph interaction in cuprates. It revealed a fine phonon structure in the electron self-energy of the underdoped $La_{2-x}Sr_xCuO_4$ samples. Remarkably, an isotope effect on the electron spectral function in Bi-2212 [108] has been discovered. These experiments together with a number of earlier optical [109, 110, 111, 112, 113, 114] and neutron-scattering [115] experimental and theoretical studies firmly established the strong coupling of carries with optical phonons in cuprates (see also Part IV).

9.2 Normal state diamagnetism: BEC versus phase fluctuations

Above T_c the charged bipolaronic Bose liquid is non-degenerate and below T_c phase coherence (ODLRO) of the preformed bosons sets in. The state above T_c is perfectly "normal" in the sense that the off-diagonal order parameter (i.e. the Bogoliubov-Gor'kov anomalous average $\mathcal{F}(\mathbf{r}, \mathbf{r}') = \langle \psi_{\downarrow}(\mathbf{r})\psi_{\uparrow}(\mathbf{r}') \rangle$) is zero above the resistive transition temperature T_c as in the BCS theory. Here $\psi_{\downarrow, \uparrow}(\mathbf{r})$ annihilates electrons with spin \downarrow, \uparrow at point \mathbf{r} .

However in contrast with the bipolaron and BCS theories a significant fraction of research in the field of cuprate superconductors suggests a so-called phase fluctuation scenario [116, 117, 118], where $\mathcal{F}(\mathbf{r}, \mathbf{r}')$ remains nonzero well above T_c . I believe that the phase fluctuation scenario is impossible to reconcile with the extremely sharp resistive transitions at T_c in high-quality underdoped, optimally doped and overdoped cuprates. For example, the in-plane and out-of-plane resistivity of Bi-2212, where the anomalous Nernst signal has been measured [117], is perfectly "normal" above T_c , Fig.8, showing only a few percent positive or negative magnetoresistance [119], explained with bipolarons [120].

Both in-plane [121, 122, 123, 124, 125] and out-of-plane [126, 127, 128] resistive transitions of high-quality samples remain sharp in the magnetic field providing a reliable determination of the genuine $H_{c2}(T)$. The preformed Cooper-pair (or phase fluctuation) model [116] is incompatible with a great number of thermodynamic, magnetic, and kinetic measurements, which show that only holes (density x), doped into a parent insulator are carriers *both*

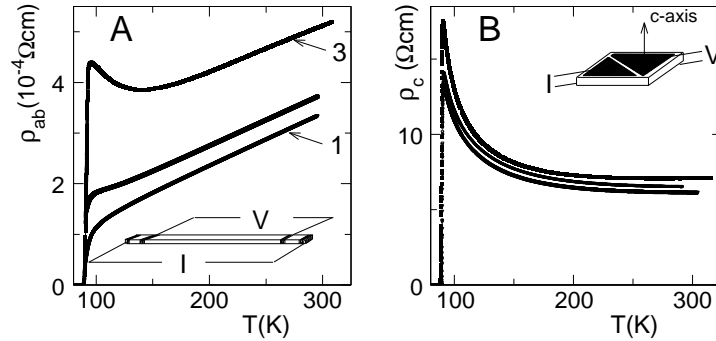


Fig. 8. In-plane (A) and out-of-plane (B) resistivity of 3 single crystals of $\text{Bi}_2\text{Sr}_2\text{CaCu}_2\text{O}_8$ [119] showing no signature of phase fluctuations well above the resistive transition.

in the normal and the superconducting states of cuprates. The assumption [116] that the superfluid density x is small compared with the normal-state carrier density is also inconsistent with the theorem [129], which proves that the number of supercarriers at $T = 0\text{K}$ should be the same as the number of normal-state carriers in any clean superfluid.

The normal state diamagnetism of cuprates provides another clear evidence for BEC rather than for the phase fluctuation scenario. A number of experiments (see, for example, [130, 131, 132, 133, 134, 118] and references therein), including torque magnetometries, showed enhanced diamagnetism above T_c , which has been explained as the fluctuation diamagnetism in quasi-2D superconducting cuprates (see, for example Ref. [132]). The data taken at relatively low magnetic fields (typically below 5 Tesla) revealed a crossing point in the magnetization $M(T, B)$ of most anisotropic cuprates (e.g. $\text{Bi} - 2212$), or in $M(T, B)/B^{1/2}$ of less anisotropic YBCO [131]. The dependence of magnetization (or $M/B^{1/2}$) on the magnetic field has been shown to vanish at some characteristic temperature below T_c . However the data taken in high magnetic fields (up to 30 Tesla) have shown that the crossing point, anticipated for low-dimensional superconductors and associated with superconducting fluctuations, does not explicitly exist in magnetic fields above 5 Tesla [133].

Most surprisingly the torque magnetometry [130, 133] uncovered a diamagnetic signal somewhat above T_c which increases in magnitude with applied magnetic field. It has been linked with the Nernst signal and mobile vortices in the normal state of cuprates [118]. However, apart from the inconsistencies mentioned above, the vortex scenario of the normal-state diamagnetism is internally inconsistent. Accepting the vortex scenario and fitting the magnetization data in $\text{Bi} - 2212$ with the conventional logarithmic field dependence [118], one obtains surprisingly high upper critical fields $H_{c2} > 120$ Tesla and a very large Ginzburg-Landau parameter, $\kappa = \lambda/\xi > 450$ even at temperatures

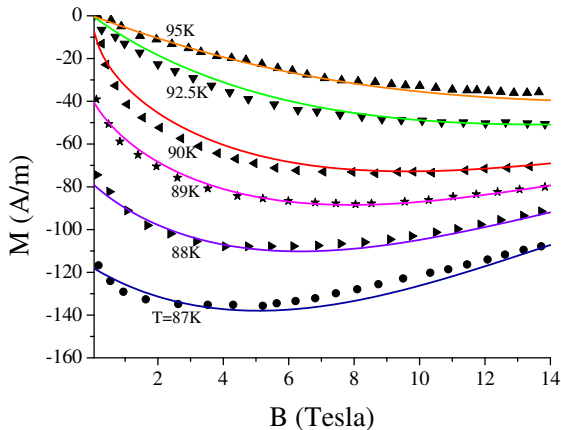


Fig. 9. Diamagnetism of optimally doped Bi-2212 (symbols)[118] compared with magnetization of CBG [95] near and above T_c (lines).

close to T_c . The in-plane low-temperature magnetic field penetration depth is $\lambda = 200$ nm in optimally doped *Bi - 2212* (see, for example [135]). Hence the zero temperature coherence length ξ turns out to be about the lattice constant, $\xi = 0.45$ nm, or even smaller. Such a small coherence length rules out the "preformed Cooper pairs" [116], since the pairs are virtually not overlapped at any size of the Fermi surface in *Bi - 2212*. Moreover the magnetic field dependence of $M(T, B)$ at and above T_c is entirely inconsistent with what one expects from a vortex liquid. While $-M(B)$ decreases logarithmically at temperatures well below T_c , the experimental curves [130, 133, 118] clearly show that $-M(B)$ increases with the field at and above T_c , just opposite to what one could expect in the vortex liquid. This significant departure from the London liquid behavior clearly indicates that the vortex liquid does not appear above the resistive phase transition [130].

Some time ago we explained the anomalous diamagnetism in cuprates as the Landau normal-state diamagnetism of preformed bosons [136]. More recently the model has been extended to high magnetic fields taking into account the magnetic pair-breaking of singlet bipolarons and the anisotropy of the energy spectrum [95]. When the magnetic field is applied perpendicular to the copper-oxygen plains the quasi-2D bipolaron energy spectrum is quantized as $E_\alpha = \omega(n + 1/2) + 2t_c[1 - \cos(K_z d)]$, where α comprises $n = 0, 1, 2, \dots$ and in-plane K_x and out-of-plane K_z center-of-mass quasi-momenta, $\omega = 2eB/\sqrt{m_x^{**}m_y^{**}}$, t_c and d are the hopping integral and the lattice period perpendicular to the planes. We assume here that the spectrum consists of two degenerate branches, so-called "x" and "y" bipolarons as in the case of apex intersite pairs [40] with anisotropic in-plane bipolaron masses

$m_x^{**} \equiv m$ and $m_y^{**} \approx 4m$. Expanding the Bose-Einstein distribution function in powers of $\exp[(\mu - E)/T]$ with the negative chemical potential μ one can after summation over n readily obtain the boson density

$$n_b = \frac{2eB}{\pi d} \sum_{r=1}^{\infty} I_0(2t_c r/T) \frac{\exp[(\mu - \omega/2 - 2t_c)r/T]}{1 - \exp(-\omega r/T)}, \quad (160)$$

and the magnetization,

$$M(T, B) = -n_b \mu_b + \frac{2eT}{\pi d} \sum_{r=1}^{\infty} I_0\left(\frac{2t_c r}{T}\right) \times \quad (161)$$

$$\frac{\exp[(\mu - \omega/2 - 2t_c)r/T]}{1 - \exp(-\omega r/T)} \left(\frac{1}{r} - \frac{\omega \exp(-\omega r/T)}{k_B T [1 - \exp(-\omega r/T)]} \right).$$

Here $\mu_b = e/\sqrt{m_x^{**} m_y^{**}}$ and $I_0(x)$ is the modified Bessel function. At low temperatures $T \rightarrow 0$ Schafroth's result [88] is recovered, $M(0, B) = -n_b \mu_b$. The magnetization of charged bosons is field-independent at low temperatures. At high temperatures, $T \gg T_c$ the chemical potential has a large magnitude, and we can keep only the terms with $r = 1$ in Eqs.(160,161) to obtain $M(T, B) = -n_b \mu_b \omega / (6T)$ at $T \gg T_c \gg \omega$, which is the familiar Landau orbital diamagnetism of nondegenerate carriers. Here T_c is the Bose-Einstein condensation temperature $T_c = 3.31(n_b/2)^{2/3} / (m_x^{**} m_y^{**} m_c^{**})^{1/3}$, with $m_c = 1/2|t_c|d^2$.

Comparing with experimental data one has to take into account a temperature and field depletion of singlets due to their thermal excitations into spin-split triplet states, $n_b(T, B) = n_c [1 - \alpha\tau - (B/B^*)^2]$. Here $\alpha = 3(2n_c t)^{-1} [J(e^{J/T_c} - 1)^{-1} - T_c \ln(1 - e^{-J/T_c})]$, $\mu_B B^* = (2T_c n_c t)^{1/2} \sinh(J/2T_c)$, $\mu_B \approx 0.93 \times 10^{-23}$ Am² is the Bohr magneton, n_c is the density of singlets at $T = T_c$ in zero field, $\tau = T/T_c - 1$, J is the singlet-triplet exchange energy, and $2t$ is the triplet bandwidth. As a result, Eq.(161) fits remarkably well the experimental curves in the critical region of optimally doped Bi-2212, Fig.9, with $n_c \mu_b = 2100$ A/m, $T_c = 90$ K, $\alpha = 0.62$ and $B^* = 56$ Tesla, which corresponds to the singlet-triplet exchange energy $J \approx 20$ K.

On the other hand the experimental data, Fig.9, contradict BCS and the phase-fluctuation scenarios [116, 118]. Indeed, if we define a critical exponent as $\delta = \ln B / \ln |M(T, B)|$ for $B \rightarrow 0$, the T dependence of $\delta(T)$ in the charged Bose gas (CBG) is dramatically different from the Berezinski-Kosterlitz-Thouless (BKT) transition critical exponents (as proposed in the phase fluctuation scenario), but it is very close to the experimental [118] $\delta(T)$, Fig.10.

Also the large Nernst signal, allegedly supporting vortex liquid in the normal state of cuprates [118], has been explained as the normal state phenomenon owing to a partial localization of charge carriers in a random potential inevitable in cuprates [98]. The coexistence of the large Nernst signal and the insulating-like resistivity in slightly doped cuprates sharply disagrees with the vortex scenario, but agrees remarkably well with our theory [99].

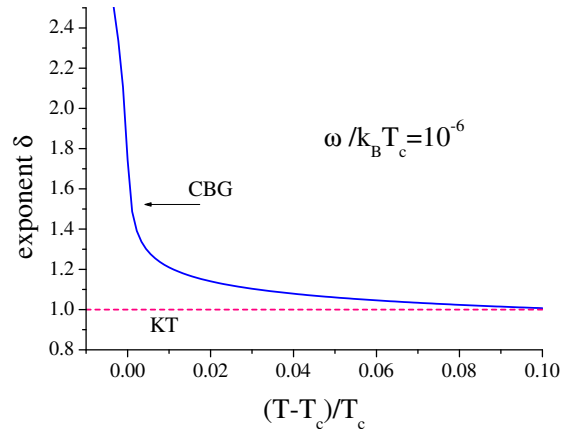


Fig. 10. Critical exponents of the low-field magnetization in CBG and in BKT transition.

9.3 Giant proximity effect

Several groups reported that in the Josephson cuprate *SNS* junctions supercurrent can run through normal *N*-barriers as thick as 100 nm in a strong conflict with the standard theoretical picture, if the barrier is made from non-superconducting cuprates. Using an advanced molecular beam epitaxy, Bozovic *et al.* [137] proved that this giant proximity effect (GPE) is intrinsic, rather than extrinsic caused by any inhomogeneity of the barrier. Hence GPE defies the conventional explanation, which predicts that the critical current should exponentially decay with the characteristic length of about the coherence length, which is $\xi \leq 1$ nm in the cuprates.

This effect can be broadly understood as the Bose-Einstein condensate tunnelling into a cuprate *semiconductor* [100]. Indeed the chemical potential μ remains in the charge-transfer gap of doped cuprates like $\text{La}_{2-x}\text{Sr}_x\text{CuO}_4$ [138] because of the bipolaron formation. The condensate wave function, $\psi(Z)$, is described by the Gross-Pitaevskii (GP) equation. In the superconducting region, $Z < 0$, near the *SN* boundary, Fig.11, the equation is

$$\frac{1}{2m_c^{**}} \frac{d^2\psi(Z)}{dZ^2} = [V|\psi(Z)|^2 - \mu]\psi(Z), \quad (162)$$

where V is a short-range repulsion of bosons, and m_c^{**} is the boson mass along Z . Deep inside the superconductor $|\psi(Z)|^2 = n_s$ and $\mu = Vn_s$, where the condensate density n_s is about $x/2$, if the temperature is well below T_c of the superconducting electrode (the in-plane lattice constant a and the unit cell volume are taken as unity).

The normal barrier at $Z > 0$ is an underdoped cuprate semiconductor above its transition temperature, where the chemical potential μ lies below the bosonic band by some energy ϵ , Fig.11. For quasi-two dimensional bosons one readily obtains [23]

$$\epsilon(T) = -T \ln(1 - e^{-T_0/T}), \quad (163)$$

where $T_0 = \pi x'/m^{**}$, m^{**} is the in-plane boson mass, and $x' < x$ is the doping level of the barrier. Then the GP equation in the barrier can be written as

$$\frac{1}{2m_c^{**}} \frac{d^2\psi(Z)}{dZ^2} = [V|\psi(Z)|^2 + \epsilon]\psi(Z). \quad (164)$$

Introducing the bulk coherence length, $\xi = 1/(2m_c^{**}n_sV)^{1/2}$ and dimensionless $f(z) = \psi(Z)/n_s^{1/2}$, $\tilde{\mu} = \epsilon/n_sV$, and $z = Z/\xi$, one obtains for a real $f(z)$

$$\frac{d^2f}{dz^2} = f^3 - f, \quad (165)$$

if $z < 0$, and

$$\frac{d^2f}{dz^2} = f^3 + \tilde{\mu}f, \quad (166)$$

if $z > 0$. These equations can be readily solved using first integrals of motion respecting the boundary conditions, $f(-\infty) = 1$, and $f(\infty) = 0$,

$$\frac{df}{dz} = -(1/2 + f^4/2 - f^2)^{1/2}, \quad (167)$$

and

$$\frac{df}{dz} = -(\tilde{\mu}f^2 + f^4/2)^{1/2}, \quad (168)$$

for $z < 0$ and $z > 0$, respectively. The solution in the superconducting electrode is given by

$$f(z) = \tanh \left[-2^{-1/2}z + 0.5 \ln \frac{2^{1/2}(1 + \tilde{\mu})^{1/2} + 1}{2^{1/2}(1 + \tilde{\mu})^{1/2} - 1} \right]. \quad (169)$$

It decays in the close vicinity of the barrier from 1 to $f(0) = [2(1 + \tilde{\mu})]^{-1/2}$ in the interval about the coherence length ξ . On the other side of the boundary, $z > 0$, it is given by

$$f(z) = \frac{(2\tilde{\mu})^{1/2}}{\sinh\{z\tilde{\mu}^{1/2} + \ln[2(\tilde{\mu}(1 + \tilde{\mu}))^{1/2} + (1 + 4\tilde{\mu}(1 + \tilde{\mu}))^{1/2}]\}}. \quad (170)$$

Its profile is shown in Fig.11. Remarkably, the order parameter penetrates into the normal layer up to the length $Z^* \approx (\tilde{\mu})^{-1/2}\xi$, which could be larger than ξ by many orders of magnitude, if $\tilde{\mu}$ is small. It is indeed the case, if the barrier layer is sufficiently doped. For example, taking $x' = 0.1$, c-axis

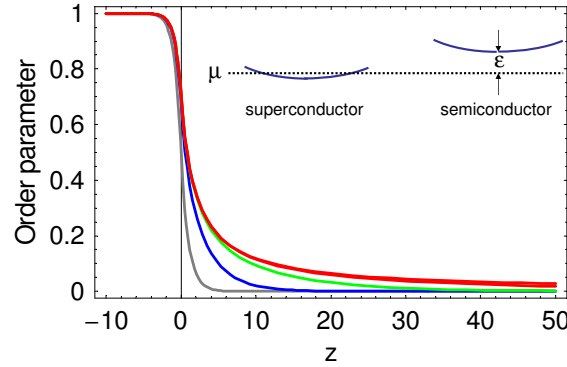


Fig. 11. BEC order parameter at the SN boundary for $\tilde{\mu} = 1.0, 0.1, 0.01$ and ≤ 0.001 (upper curve).

$m_c^{**} = 2000m_e$, in-plane $m^{**} = 10m_e$ [23], $a = 0.4$ nm, and $\xi = 0.6$ nm, yields $T_0 \approx 140$ K and $(\tilde{\mu})^{-1/2} \approx 5000$ at $T = 10$ K. Hence the order parameter could penetrate into the normal cuprate semiconductor up to more than a thousand coherence lengths as observed [137]. If the thickness of the barrier L is small compared with Z^* , and $(\tilde{\mu})^{1/2} \ll 1$, the order parameter decays following the power law, rather than exponentially,

$$f(z) = \frac{\sqrt{2}}{z+2}. \quad (171)$$

Hence, for $L \leq Z^*$, the critical current should also decay following the power law [100]. On the other hand, for an *undoped* barrier $\tilde{\mu}$ becomes larger than unity, $\tilde{\mu} \propto \ln(m^{**}T/\pi x') \rightarrow \infty$ for any finite temperature T when $x' \rightarrow 0$, and the current should exponentially decay with the characteristic length smaller than ξ , as is experimentally observed as well [138]. As a result the bipolaron theory accounts for the giant and nil proximity effects in slightly doped semiconducting and undoped insulating cuprates, respectively. It predicts the occurrence of a new length scale, $\hbar/\sqrt{2m_c^{**}\epsilon(T)}$, and explains the temperature dependence of the critical current of SNS junctions [100].

10 Conclusion

Extending the BCS theory towards the strong interaction between electrons and ion vibrations, a charged Bose gas of tightly bound small bipolarons was

predicted by us [41] with a further prediction that high T_c should exist in the crossover region of the e-ph interaction strength from the BCS-like to bipolaronic superconductivity [18].

For very strong electron-phonon coupling, polarons become self-trapped on a single lattice site. The energy of the resulting small polaron is given as $-E_p = -\lambda zt$. Expanding about the atomic limit in hopping integrals t (which is small compared to E_p in the small polaron regime, $\lambda > 1$) the polaron mass is computed as $m^* = m_0 \exp(\gamma E_p/\omega_0)$, where ω_0 is the frequency of Einstein phonons, m_0 is the rigid band mass on a cubic lattice, and γ is a numerical constant. For the Holstein model, which is purely site local, $\gamma = 1$. Bipolarons are on-site singlets in the Holstein model and their mass m_H^{**} appears only in the second order of t [41] scaling as $m_H^{**} \propto (m^*)^2$ for $\omega \gg \Delta$, and as $m_H^{**} \propto (m^*)^4$ in a more realistic regime $\omega \ll \Delta$ (section 7). Here $\Delta = 2E_p - U$ is the bipolaron binding energy, and U is the on-site (Hubbard) repulsion. Since the Hubbard U is about 1 eV or larger in strongly correlated materials, the electron-phonon coupling must be large to stabilize on-site bipolarons and the Holstein bipolaron mass appears very large, $m_H^{**}/m_0 > 1000$, for realistic values of the phonon frequency.

This estimate led some authors to the conclusion that the formation of itinerant small polarons and bipolarons in real materials is unlikely [140], and high-temperature bipolaronic superconductivity is impossible [141]. However, one should note that the Holstein model is an extreme polaron model, and typically yields the highest possible value of the (bi)polaron mass in the strong coupling limit. Many advanced materials with low density of free carriers and poor mobility (at least in one direction) are characterized by poor screening of high-frequency optical phonons and are more appropriately described by the long-range Fröhlich electron-phonon interaction [40]. For this interaction the parameter γ is less than 1 ($\gamma \approx 0.3$ on the square lattice and $\gamma \approx 0.2$ on the triangular lattice), reflecting the fact that in a hopping event the lattice deformation is partially pre-existent. Hence the unscreened Fröhlich electron-phonon interaction provides relatively light small polarons, which are several orders of magnitude lighter than small Holstein polarons.

As shown above FCM is reduced to an extended Hubbard model with intersite attraction and suppressed double-occupancy in the limit of high phonon frequency $\omega \geq t$ and large on-site Coulomb repulsion. Then the Hamiltonian can be projected onto the subspace of nearest neighbor intersite bipolarons. In contrast with the crawler motion of on-site bipolaron, the intersite bipolaron tunnelling is a crab-like, so that its mass scales linearly with the polaron mass ($m^{**} \approx 4m^*$ on the staggered chain [80]) as confirmed numerically using CTQMC algorithm by Kornilovitch [42]. As a result, the crab bipolarons could bose-condense already at the room temperature [70].

We believe that the following recipe is worth investigating to look for room-temperature superconductivity [70]: (a) The parent compound should be an ionic insulator with light ions to form high-frequency optical phonons, (b) The structure should be quasi two-dimensional to ensure poor screening of

high-frequency *c*-axis polarized phonons, (c) A triangular lattice is desirable in combination with strong, on-site Coulomb repulsion to form the superlight crab bipolaron, and (d) Moderate carrier densities are required to keep the system of small bipolarons close to the dilute regime. I believe that most of these conditions are already met in cuprate superconductors. As discussed above there is strong evidence for 3D bipolaronic BEC in cuprates from unusual upper critical fields and the electronic specific heat, normal state pseudogaps and anisotropy, normal state diamagnetism, the Hall-Lorenz numbers, and the giant proximity effect.

Acknowledgements

I thank A. F. Andreev, J. P. Hague, V. V. Kabanov, P. E. Kornilovitch, and J. H. Samson for illuminating discussions and collaboration. The work was supported by EPSRC (UK) (grant no. EP/C518365/1).

References

1. A. S. Alexandrov and N. F. Mott, Rep. Prog. Phys. **57**, 1197 (1994); *'Polarons and Bipolarons'* (World Scientific, Singapore, 1995).
2. J. T. Devreese, in *Encyclopedia of Applied Physics* (VCH Publishers, 1996), vol. 14, p. 383; *Polaron* (In Encyclopedia of Physics, vol. 2, ed by R.G. Lerner, G. L. Trigg, Wiley-VCH, Weinheim, 2005) p. 2004.
3. J. T. Devreese, in the present volume.
4. E. I. Rashba, in *Encyclopedia of Condensed Matter Physics*, eds. G. F. Bassani, G. L. Liedl, and P. Wyder (Elsevier, 2005), p. 347.
5. *Anharmonic Properties of High- T_c Cuprates*, eds. D. Mihailović *et al.*, (World Scientific, Singapore, 1995).
6. *Polarons and Bipolarons in High- T_c Superconductors and Related Materials*, eds E. K. H. Salje, A. S. Alexandrov and W. Y. Liang (Cambridge University Press, Cambridge, 1995).
7. N. Itoh and A. M. Stoneham, *Materials Modification by Electronic Excitation* (Cambridge University Press, Cambridge, 2001).
8. J. Appel, in *Solid State Physics* **21**(eds. F. Seitz, D. Turnbull, and H. Ehrenreich, Academic Press, 1968).
9. Yu. A. Firsov (ed) *Polarons* (Nauka, Moscow, 1975).
10. H. Boettger and V.V. Bryksin, *Hopping Conduction in Solids* (Akademie-Verlag, Berlin, 1985).
11. A. B. Migdal, Zh. Eksp. Teor. Fiz. **34**, 1438 (1958) [Sov. Phys. JETP **7**, 996 (1958)].
12. J. Bardeen, L. N. Cooper, and J. R. Schrieffer, Phys. Rev. **108**, 1175 (1957).
13. G. M. Eliashberg, Zh. Eksp. Teor. Fiz. **38**, 966 (1960); **39**, 1437 (1960) [Sov. Phys. JETP **11**, 696; **12**, 1000 (1960)].
14. D. J. Scalapino, in *Superconductivity*, ed. R. D. Parks (Marcel Dekker, NY, 1069), p. 449.

15. A. S. Alexandrov, V. N. Grebenev, and E. A. Mazur, Pis'ma Zh. Eksp. Teor. Fiz. **45**, 357 (1987)[JETP Lett. **45**, 455 (1987)].
16. F. Dogan and F. Marsiglio, Phys. Rev. **B68**, 165102 (2003).
17. J. P. Hague, J. Phys.: Condens. Mat. **15**, 2535 (2003), and references therein.
18. A. S. Alexandrov, Zh. Fiz. Khim. **57**, 273 (1983) (Russ. J. Phys. Chem. **57**, 167 (1983)).
19. I. G. Lang and Yu. A. Firsov, Zh. Eksp. Teor. Fiz. **43**, 1843 (1962) [Sov. Phys. JETP **16**, 1301 (1963)].
20. A. S. Alexandrov, Phys. Rev. B **46**, 2838 (1992).
21. A. S. Alexandrov, in *Models and Phenomenology for Conventional and High-Temperature Superconductivity*, Course CXXXVI of the International School of Physics 'Enrico Fermi', eds. G. Iadonisi, J. R. Schrieffer, and M. L. Chiofalo, (IOS Press, Amsterdam, 1998) p 309.
22. A. S. Alexandrov, Europhys. Lett., **56**, 92 (2001).
23. A. S. Alexandrov, *Theory of Superconductivity: From Weak to Strong Coupling* (IoP Publishing, Bristol, 2003).
24. L. D. Landau, Physikalische Zeitschrift der Sowjetunion, **3**, 664 (1933).
25. V. V. Kabanov and O. Yu. Mashtakov, Phys. Rev. B **47**, 6060 (1993).
26. A. S. Alexandrov, V. V. Kabanov, and D. K. Ray, Phys. Rev. B **49**, 9915 (1994).
27. H. Fehske, H. Röder, G. Wellein, and A. Mistryotis, Phys. Rev. B **51**, 16582 (1995); G. Wellein, H. Röder, and H. Fehske, Phys. Rev. B **53**, 9666 (1996).
28. F. Marsiglio, Physica C **244**, 21 (1995).
29. Y. Takada and T. Higuchi, Phys. Rev. B **52**, 12720 (1995).
30. H. Fehske, J. Loos, and G. Wellein, Z. Phys. **B104**, 619 (1997).
31. T. Hotta and Y. Takada, Phys. Rev. B **56**, 13 916 (1997).
32. A. H. Romero, D. W. Brown and K. Lindenberg, J. Chem. Phys. **109**, 6504 (1998); Phys. Rev. B **59**, 13728 (1999); Phys. Rev. B **60**, 4618 (1999); Phys. Rev. B **60**, 14080 (1999).
33. A. La Magna and R. Pucci, Phys. Rev. B **53**, 8449 (1996).
34. P. Benedetti and R. Zeyher, Phys. Rev. B **58**, 14320 (1998).
35. T. Frank and M. Wagner, Phys. Rev. B **60**, 3252 (1999).
36. L. Proville and S. Aubry, S. Eur. Phys. J. B **11**, 41 (1999).
37. J. Bonča, S. A. Trugman, and I. Batistić, Phys. Rev. B **60**, 1633 (1999); J. Bonča, T. Katrasnic, and S. A. Trugman, Phys. Rev. Lett. **84**, 3153 (2000); L.-C. Ku, S. A. Trugman, and J. Bonča, Phys. Rev. B **65**, 174306 (2002); S. El Shawish, J. Bonča, L.-C. Ku, and S. A. Trugman, Phys. Rev. B **67**, 014301 (2003).
38. A. S. Alexandrov and P. E. Kornilovitch, Phys. Rev. Lett. **82**, 807 (1999).
39. A. S. Alexandrov, Phys. Rev. B **61**, 12315 (2000).
40. A. S. Alexandrov, Phys. Rev. B **53**, 2863 (1996).
41. A. S. Alexandrov and J. Ranninger, Phys. Rev. B **23**, 1796 (1981), *ibid* **24**, 1164 (1981).
42. P. Kornilovitch, in the present volume.
43. R. T. Shuey, Phys. Rev. A, **139**, 1675 (1994).
44. E. G. Maximov, D. Yu. Savrasov, and S. Yu. Savrasov, Uspechi Fiz. Nauk., **167**, 353 (1997).
45. V. G. Baryakhtar, E. V. Zaroquentsev, and E. P. Troitskaya *Theory of Adiabatic Potential and Atomic Properties of Simple Metals* (Gordon and Breach, Amsterdam, 1999).

46. G. D. Mahan, *Many-Particle Physics* (Plenum Press, New York, 1990).
47. V.V. Kabanov, in the present volume.
48. B.T. Geilikman, *Usp. Fiz. Nauk* **115**, 403 (1975) [*Sov. Phys. Usp.* **18**, 190 (1975)].
49. T. Holstein, *Ann. Phys.* **8**, 325; 343 (1959).
50. E. I. Rashba, *Opt. Spectr.* **2**, 75 (1957); *Excitons*, eds. E. I. Rashba and D. M. Struge (Nauka, Moscow, 1985).
51. P. W. Anderson, *Phys. Rev. Lett.* **34**, 953 (1975).
52. S. Aubry, in the present volume.
53. H. Hiramoto and Y. Toyozawa, *J. Phys. Soc. Jpn.* **54**, 245 (1985).
54. J. Ranninger and U. Thibblin, *Phys. Rev. B* **45**, 7730 (1992).
55. E. V. L. de Mello and J. Ranninger, *Phys. Rev. B* **55**, 14872 (1997).
56. E. V. L. de Mello and J. Ranninger, *Phys. Rev. B* **58**, 9098 (1998).
57. E. K. Kudinov and Yu. A. Firsov, *Fiz. Tverd. Tela (S.-Peterburg)* **39**, 2159 (1997) [*Phys. Solid State* **39**, 1930 (1997)].
58. Yu. A. Firsov, E. K. Kudinov, V. V. Kabanov, and A. S. Alexandrov, *Phys. Rev. B* **59**, 12132 (1999).
59. A. S. Alexandrov, *Phys. Rev. B* **61**, 315 (2000).
60. D. M. Eagles, *Phys. Rev.* **130**, 1381 (1963); *Phys. Rev.* **181**, 1278 (1969); *Phys. Rev.* **186**, 456 (1969).
61. A. A. Gogolin, *Phys. Status Solidi B* **109**, 95 (1982).
62. V. Cataudella, G. De Filippis, and C.A. Perroni, in the present volume.
63. H. Fehske and S. A. Trugman, in the present volume.
64. H. de Raedt and A. Lagendijk, *Phys. Rev. Lett.* **49**, 1522 (1982); *Phys. Rev. B* **27**, 6097 (1983); *Phys. Rev. B* **30**, 1671 (1984); *Phys. Rep.* **127**, 234 (1985).
65. M. Hohenadler, H. G. Evertz, and W. von der Linden, *Phys. Rev. B* **69**, 024301 (2004).
66. A. S. Mishchenko, N.V. Prokof'ev, A. Sakamoto, and B.V. Svistunov, *Phys. Rev. B* **62**, 6317 (2000); A. S. Mishchenko, N. Nagaosa, N. V. Prokof'ev, A. Sakamoto, and B. V. Svistunov, *Phys. Rev. Lett.* **91**, 236401 (2003).
67. A. Macridin, G. A. Sawatzky, and M. Jarrell, *Phys. Rev. B* **69**, 245111 (2004).
68. P. E. Spencer, J. H. Samson, P. E. Kornilovitch, and A. S. Alexandrov, *Phys. Rev. B* **71**, 184319 (2005).
69. J. P. Hague, P. E. Kornilovitch, A. S. Alexandrov, and J. H. Samson, *Phys. Rev. B* **73**, 054303 (2006).
70. J. P. Hague, P. E. Kornilovitch, J. H. Samson, and A. S. Alexandrov, *Phys. Rev. Lett.* **98**, 037002 (2007) .
71. A. S. Mishchenko and N. Nagaosa, this volume.
72. M. Zoli, *Phys. Rev. B* **57**, 555 (1998); *ibid* **61**, 14523 (2000).
73. A. S. Alexandrov and C. Sricheewin, *Europhys. Lett.* **51**, 188 (2000).
74. A. S. Alexandrov and J. Ranninger, *Phys. Rev. B* **45**, 13109 (1992); *Physica C* **198**, 360 (1992).
75. H. Fröhlich, *Adv. Phys.* **3**, 325 (1954).
76. V. L. Vinetskii and M. Sh. Giterman, *Zh. Eksp. Teor. Fiz.* **33**, 730 (1957) [*Sov. Phys. JETP* **6**, 560 (1958)].
77. G. Verbist, F. M. Peeters, and J. T. Devreese, *Phys. Rev. B* **43**, 2712 (1991); *Solid State Commun.* **76**, 1005 (1990).
78. A. S. Alexandrov(Aleksandrov) and V. V. Kabanov, *Fiz. Tverd. Tela* **28**, 1129 (1986) [*1986 Soviet Phys. Solid St.* **28**, 631 (1986)].

79. V. V. Bryksin and A. V. Gol'tsev, *Fiz. Tverd. Tela* **30**, 1476 (1988) [*Sov. Phys. Solid State* **30**, 851 (1988)].
80. A. S. Alexandrov and P. E. Kornilovitch, *J. Phys.: Condens. Matter* **14**, 5337 (2002).
81. J. Bonča and S. A. Trugman, *Phys. Rev B* **64**, 094507 (2001).
82. C. R. A. Catlow, M. S. Islam and X. Zhang, *J. Phys.: Condens. Matter* **10**, L49 (1998).
83. A. S. Alexandrov and V. V. Kabanov, *JETP Lett.* **72**, 569 (2000).
84. T. Mertelj, V. V. Kabanov, and D. Mihailovic, *Phys. Rev. Lett.* **94**, 147003 (2005).
85. A. S. Alexandrov, J. Ranninger, and S. Robaszkiewicz, *Phys. Rev. B* **33**, 4526 (1986).
86. A. S. Alexandrov, D. A. Samarchenko, and S. V. Traven, *Zh. Eksp. Teor. Fiz.* **93**, 1007 (1987) [*Sov. Phys. JETP* **66**, 567 (1987)].
87. R. E. Peierls, *Z. Phys.* **80**, 763 (1933).
88. M. R. Schafroth, *Phys. Rev.* **100**, 463 (1955); J. M. Blatt and S. T. Butler, *Phys. Rev.* **100**, 476 (1955).
89. A. S. Alexandrov, Doctoral Thesis MEPHI (Moscow, 1984); *Phys. Rev. B* **48**, 10571 (1993).
90. A. S. Alexandrov, W. H. Beere, V. V. Kabanov, and W. Y. Liang, *Phys. Rev. Lett.* **79**, 1551 (1997).
91. A. S. Alexandrov, *Phys. Rev. Lett.* **82**, 2620 (1999); A. S. Alexandrov and V. V. Kabanov, *Phys. Rev. B* **59**, 13628 (1999).
92. A. S. Alexandrov, *J. Low Temp. Phys.* **87**, 721 (1992).
93. D. Mihailovic, V. V. Kabanov, K. Zagar, and J. Demsar, *Phys. Rev. B* **60**, 6995 (1999) and references therein.
94. A. S. Alexandrov, V. V. Kabanov, and N. F. Mott, *Phys. Rev. Lett.* **77**, 4796 (1996).
95. A. S. Alexandrov, *Phys. Rev. Lett.* **96**, 147003 (2006).
96. K. K. Lee, A. S. Alexandrov, and W. Y. Liang, *Phys. Rev. Lett.* **90**, 217001 (2003); *Eur. Phys. J.* **B30**, 459 (2004).
97. A. S. Alexandrov, *Phys. Rev. B* **73**, 100501 (2006).
98. A. S. Alexandrov and V. N. Zavaritsky, *Phys. Rev. Lett.* **93**, 217002 (2004).
99. A. S. Alexandrov, *Phys. Rev. Lett.* **95**, 259704 (2005).
100. A.S. Alexandrov, cond-mat/0607770.
101. V. N. Zavaritsky, V. V. Kabanov, A. S. Alexandrov, *Europhys. Lett.* **60**, 127 (2002).
102. Y. Zhang, N. P. Ong, Z. A. Xu, K. Krishana, R. Gagnon, L. Taillefer, *Phys. Rev. Lett.* **84**, 2219 (2000).
103. A. S. Alexandrov, N. F. Mott, *Phys. Rev. Lett.* **1993**, 71, 1075.
104. G. Zhao and D. E. Morris, *Phys. Rev. B* **51**, 16487 (1995); G.-M. Zhao, M. B. Hunt, H. Keller, and K. A. Müller, *Nature* **385**, 236 (1997); R. Khasanov, D. G. Eshchenko, H. Luetkens, E. Morenzoni, T. Prokscha, A. Suter, N. Garifianov, M. Mali, J. Roos, K. Conder, and H. Keller *Phys. Rev. Lett.* **92**, 057602 (2004).
105. in the present volume.
106. A. S. Alexandrov, *Phys. Rev. B* **46**, 14932 (1992).
107. A. Lanzara, P. V. Bogdanov, X. J. Zhou, S. A. Kellar, D. L. Feng, E. D. Lu, T. Yoshida, H. Eisaki, A. Fujimori, K. Kishio, J. I. Shimoyana, T. Noda, S. Uchida, Z. Hussain, Z. X. Shen, *Nature* **2001**, 412, 510.

108. G. H. Gweon, T. Sasagawa, S. Y. Zhou, J. Craf, H. Takagi, D. H. Lee, A. Lanzara, *Nature* **2004**, 430, 187.
109. D. Mihailovic, C.M. Foster, K. Voss, and A.J. Heeger, *Phys. Rev. B* **42**, 7989 (1990).
110. P. Calvani, M. Capizzi, S. Lupi, P. Maselli, A. Paolone, P. Roy, S.W. Cheong, W. Sadowski, and E. Walker, *Solid State Commun.* **91**, 113 (1994).
111. R. Zamboni, G. Ruani, A.J. Pal, and C. Taliani, *Solid St. Commun.* **70**, 813 (1989).
112. T. Timusk, C.C. Homes, and W. Reichardt, in *Anharmonic properties of High Tc cuprates* (eds. D. Mihailovic, G. Ruani, E. Kaldis, and K.A. Müller, World Scientific, Singapore, 1995) p.171.
113. J. Tempere and J. T. Devreese, *Phys. Rev. B* **64**, 104504 (2001).
114. J. T. Devreese, in the present volume.
115. T.R. Sendyka, W. Dmowski, and T. Egami, *Phys. Rev. B* **51**, 6747 (1995); T. Egami, *J. Low Temp. Phys.* **105**, 791 (1996).
116. V. J. Emery and S. A. Kivelson, *Nature (London)*, **374**, 434 (1995).
117. Z. A. Xu, N. P. Ong, Y. Wang, T. Kakeshita, and S. Uchida, *Nature (London)* **406**, 486 (2000); N. P. Ong and Y. Wang, *Physica C* **408**, 11 (2004).
118. Y. Wang, L. Li, M. J. Naughton, G.D. Gu, S. Uchida, and N. P. Ong, *Phys. Rev. Lett.* **95**, 247002 (2005); L. Li, Y. Wang, M. J. Naughton, S. Ono, Y. Ando, and N. P. Ong, *Europhys. Lett.* **72**, 451(2005); Y. Wang, L. Li, and N. P. Ong, *Phys. Rev. B* **73**, 024510 (2006).
119. V. N. Zavaritsky and A. S. Alexandrov, *Phys. Rev. B* **71**, 012502 (2005).
120. V. N. Zavaritsky, J. Vanacken, V. V. Moshchalkov, and A. S. Alexandrov, *Eur. Phys. J. B* **42**, 367 (2004).
121. B. Bucher, J. Karpinski, E. Kaldis, and P. Wachter, *Physica C* **167**, 324 (1990).
122. A. P. Mackenzie, S. R. Julian, G. G. Lonzarich, A. Carrington, S. D. Hughes, R. S. Liu, and D. C. Sinclair, *Phys. Rev. Lett.* **71**, 1238 (1993)
123. M. A. Osofsky, R. J. Soulen, A. A. Wolf, J. M. Broto, H. Rakoto, J. C. Ousset, G. Coffe, S. Askenazy, P. Pari, I. Bozovic, J. N. Eckstein, and G. F. Virshup, *Phys. Rev. Lett.* **71**, 2315 (1993); *ibid* **72**, 3292 (1994).
124. D. D. Lawrie, J. P. Franck, J. R. Beamish, E. B. Molz, W. M. Chen, and M. J. Graf, *J. Low Temp. Phys.* **107**, 491 (1997).
125. V. F. Gantmakher, G. E. Tsydynzhapov, L. P. Kozeeva, and A. N. Lavrov, *Zh. Eksp. Teor. Fiz.* **88**, 148 (1999).
126. A. S. Alexandrov, V. N. Zavaritsky, W. Y. Liang, and P. L. Nevsky, *Phys. Rev. Lett.* **76**, 983 (1996).
127. J. Hofer, J. Karpinski, M. Willemin, G. I. Meijer, E. M. Kopnin, R. Molinski, H. Schwer, C. Rossel, and H. Keller, *Physica C* **297**, 103 (1998).
128. V. N. Zverev and D. V. Shovkun, *JETP Lett.* **72**, 73 (2000).
129. A. J. Leggett, *Physica Fennica* **8**, 125 (1973); *J Stat. Phys.* **93**, 927 (1998); V. N. Popov, *Functional Integrals and Collective Excitations* (Cambridge University Press, Cambridge, 1987).
130. C. Bergemann, A. W. Tyler, A. P. Mackenzie, J. R. Cooper, S. R. Julian, and D. E. Farrel, *Phys. Rev. B* **57**, 14387 (1998).
131. A. Junod, J-Y. Genouda, G. Triscone, and T. Schneider, *Physica C* **294**, 115 (1998).
132. J. Hofer, T. Schneider, J. M. Singer, M. Willemin, H. Keller, T. Sasagawa, K. Kishio, K. Conder, and J. Karpinski, *Phys. Rev. B* **62**, 631 (2000).

133. M. J. Naughton, Phys. Rev. B **61**, 1605 (2000).
134. I. Iguchi, A. Sugimoto, and H. Sato, J. Low Temp. Phys. **131**, 451 (2003).
135. J. L. Tallon, J. W. Loram, J. R. Cooper, C. Panagopoulos, and C. Bernhard, Phys. Rev. B **68**, 180501(R) (2003).
136. C. J. Dent, A. S. Alexandrov, and V. V. Kabanov, Physica C **341-348**, 153 (2000).
137. I. Bozovic, G. Logvenov, M. A. J. Verhoeven, P. Caputo, E. Goldobin, and M. R. Beasley, Phys. Rev. Lett. **93**, 157002 (2004).
138. I. Bozovic, G. Logvenov, M. A. J. Verhoeven, P. Caputo, E. Goldobin, and T. H. Geballe, Nature (London) **422**, 873 (2003)
139. R. A. Ogg Jr., Phys. Rev. **69**, 243 (1946).
140. E. V. L. de Mello and J. Ranninger, Phys. Rev. B **58**, 9098 (1998).
141. P. W. Anderson, *The Theory of Superconductivity in the Cuprates* (Princeton University Press, Princeton NY, 1997).